Department of Radio Science and Engineering

Integral equation methods for extreme-parameter materials and novel boundary conditions

Johannes Markkanen

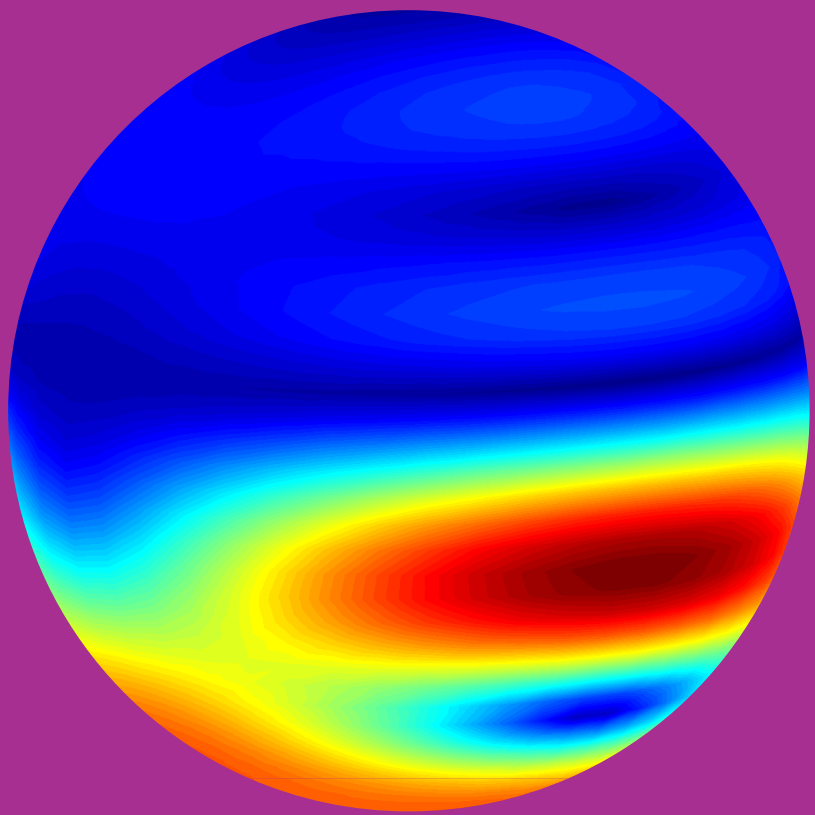

Aalto University

DOCTORAL DISSERTATIONS

Aalto University publication series
DOCTORAL DISSERTATIONS 109/2013

Integral equation methods for extreme-parameter materials and novel boundary conditions

Johannes Markkanen

A doctoral dissertation completed for the degree of Doctor of Science (Technology) to be defended, with the permission of the Aalto University School of Electrical Engineering, at a public examination held at the lecture hall S1 of the school on 8 August 2013 at 12.

Aalto University
School of Electrical Engineering
Department of Radio Science and Engineering
Electromagnetics

Supervising professor
Professor Ari Sihvola

Thesis advisor
Doctor Pasi Ylä-Oijala

Preliminary examiners
Professor Francesco Andriulli, Telecom Bretagne, France
Professor Stefano Maci, University of Siena, Italy

Opponent
Professor Ali E. Yilmaz, The University of Texas at Austin, USA

Aalto University publication series
DOCTORAL DISSERTATIONS 109/2013

ISBN 978-952-60-5242-7 (printed)
ISBN 978-952-60-5243-4 (pdf)
ISSN-L 1799-4934
ISSN 1799-4934 (printed)
ISSN 1799-4942 (pdf)
http://urn.fi/URN:ISBN:978-952-60-5243-4

http://lib.tkk.fi/Diss/

Unigrafia Oy
Helsinki 2013

Finland

441 697
Printed matter

Aalto University

Abstract

Aalto University, P.O. Box 11000, FI-00076 Aalto www.aalto.fi

Author
Johannes Markkanen

Name of the doctoral dissertation
Integral equation methods for extreme-parameter materials and novel boundary conditions

Publisher School of Electrical Engineering

Unit Department of Radio Science and Engineering

Series Aalto University publication series DOCTORAL DISSERTATIONS 109/2013

Field of research Electromagnetics

Manuscript submitted 4 March 2013 **Date of the defence** 8 August 2013

Permission to publish granted (date) 16 May 2013 **Language** English

☐ **Monograph** ☒ **Article dissertation (summary + original articles)**

Abstract

This thesis aims to develop accurate and efficient numerical methods for modeling electromagnetic properties of materials with extreme parameters and nonconventional boundary conditions. Materials with the permittivity and permeability dyadics being strongly inhomogeneous or anisotropic or having parameters near zero or infinity are considered as extreme materials. Nonconventional boundary conditions investigated in this thesis are called DB and D′B′ boundary conditions, which require the vanishing of the normal components of the fluxes (DB) or their normal derivatives (D′B′).

This thesis consists of three main topics. In the first part, a surface integral equation-based solution for electromagnetic wave scattering by objects with the DB boundary condition is developed. The integral equations are solved by the method of moments. The DB boundary condition is enforced by restricting the freedom of the unknown surface current densities. The developed method is then used for analyzing electromagnetic scattering by the ideal DB objects.

The second part examines properties of different volume integral equation formulations and their discretizations. The accuracy and stability of these formulations are analyzed when the material parameters are complicated or pushed to the extreme limits. It is shown that the formulation with the equivalent volume currents as unknowns is more stable than the conventional ones when the material parameters are extremely anisotropic.

The third part focuses on material approximations of the DB and D′B′ boundary conditions in terms of an interface against some extreme-parameter material. Scattering properties of these approximations are investigated by using the volume integral equation method developed in the second part.

Keywords integral equation methods, method of moments, DB boundary condition, D′B′ boundary condition, anisotropy, extereme materials

ISBN (printed) 978-952-60-5242-7 **ISBN (pdf)** 978-952-60-5243-4

ISSN-L 1799-4934 **ISSN (printed)** 1799-4934 **ISSN (pdf)** 1799-4942

Location of publisher Espoo **Location of printing** Helsinki **Year** 2013

Pages 118 **urn** http://urn.fi/URN:ISBN:978-952-60-5243-4

Aalto-yliopisto

Tiivistelmä

Aalto-yliopisto, PL 11000, 00076 Aalto www.aalto.fi

Tekijä
Johannes Markkanen

Väitöskirjan nimi
Integraaliyhtälömenetelmät äärimmäisille materiaaleille ja uusille reunaehdoille

Julkaisija Sähkötekniikan korkeakoulu

Yksikkö Radiotieteen ja -tekniikan laitos

Sarja Aalto University publication series DOCTORAL DISSERTATIONS 109/2013

Tutkimusala Sähkömagnetiikka

Käsikirjoituksen pvm 04.03.2013 **Väitöspäivä** 08.08.2013

Julkaisuluvan myöntämispäivä 16.05.2013 **Kieli** Englanti

☐ **Monografia** ☒ **Yhdistelmäväitöskirja (yhteenveto-osa + erillisartikkelit)**

Tiivistelmä

Väitöskirjan tavoitteena on kehittää tarkkoja ja tehokkaita numeerisia menetelmiä mallintamaan materiaalien sähkömagneettisia ominaisuuksia. Työssä tutkitaan materiaaleja, joiden sähkömagneettista vastetta kuvaavat parametrit permittiivisyys ja permeabiilisuus voivat olla voimakkaasti riippuvaisia kentän suunnasta tai saada äärimmäisiä arvoja. Lisäksi työssä tutkitaan erikoisia niin sanottuja DB ja D′B′ reunaehtoja, jotka rajoittavat kenttien normaalikomponenttien tai niiden normaali derivaattojen käyttäytymistä.

Väitöskirja voidaan karkeasti jakaa kolmeen osaan. Ensimmäisessä osassa kehitetään pintaintegraaliyhtälöihin perustuvia laskennallisia menetelmiä sähkömagneettisten sirontaongelmien ratkaisemiseksi kappaleista, joiden pinnalla DB reunaehto on voimassa. Menetelmässä DB reunaehto pakotetaan voimaan rajoittamalla tuntemattomien pintavirtatiheyksien käyttäytymistä kappaleen pinnalla. Lisäksi tutkitaan DB kappaleiden sähkömagneettisia sirontaominaisuuksia.

Toisessa osassa tarkastellaan tilavuusintegraaliyhtälömenetelmien ominaisuuksia. Erityisesti perehdytään diskretoitujen yhtälöiden tarkkuuteen ja stabiilisuuteen kun materiaaliparametrit lähestyvät äärimmäisiä arvoja. Työssä näytetään että tilavuusvirtoihin perustuva formulaatio käyttäytyy paremmin kuin tavanomaiset formulaatiot kun materiaaliparametrit ovat voimakkaasti epäsotrooppisia.

Lopuksi väitöskirja käsittelee DB ja D′B′ reunaehtojen realisointia sähkömagneettisten materiaaliparametrien avulla. Realisaatiot vaativat voimakkaasti epäisotrooppisia materiaaleja, joiden laskennalliseen mallintamiseen käytetään toisessa osassa kehitettyä menetelmää.

Avainsanat integraaliyhtälömenetelmät, momenttimenetelmä, DB reunaehto, D′B′ reunaehto, anisotropia, äärimmäiset materiaalit

ISBN (painettu) 978-952-60-5242-7 **ISBN (pdf)** 978-952-60-5243-4

ISSN-L 1799-4934 **ISSN (painettu)** 1799-4934 **ISSN (pdf)** 1799-4942

Julkaisupaikka Espoo **Painopaikka** Helsinki **Vuosi** 2013

Sivumäärä 118 **urn** http://urn.fi/URN:ISBN:978-952-60-5243-4

Preface

This thesis was carried out at the Department of Radio Science and Engineering, Aalto University School of Electrical Engineering during 2010-2013.

First of all, I would like to thank my supervisor Professor Ari Sihvola and my instructor Doctor Pasi Ylä-Oijala for giving me the opportunity to work with this interesting topic and also I would like to thank them for all guidance and help that I have received throughout these years. My gratitude belongs to my co-authors, colleagues, and all staff members in the Department of Radio Science and Engineering, as well as pre-examiners of this thesis Professor Francesco Andriulli and Professor Stefano Maci for their effort in reviewing this thesis.

Special thanks belong to one of my co-author Professor Cai-Cheng Lu, who also invited me for a five-month research visit to the Department of Electrical and Computer Engineering of the University of Kentucky.

For financial support, I thank the Graduate School in Electronics, Telecommunication and Automation (GETA), the Academy of Finland, and the Cultural Foundation of Finland.

Finally, I wish thank my family and friends who have always been interested in my research and asked lots of difficult questions.

Espoo, June 17, 2013,

Johannes Markkanen

Contents

List of Publications

This thesis consists of an overview and of the following publications which are referred to in the text by their Roman numerals.

I J. Markkanen, P. Ylä-Oijala, and A. Sihvola. Computation of scattering by DB objects with surface integral equation method. *IEEE Transactions on Antennas and Propagation*, vol. 59, no. 1, pp. 154–161, January 2011.

II J. Markkanen, P. Ylä-Oijala, and A. Sihvola. Surface integral equation method for scattering by DB objects with sharp wedges. *ACES Journal*, vol. 26, no. 5, pp. 367–374, May 2011.

III J. Markkanen, C-C. Lu, X. Cao, and P. Ylä-Oijala. Analysis of volume integral equation formulations for scattering by high-contrast penetrable objects. *IEEE Transactions on Antennas and Propagation*, vol. 60, no. 5, pp. 2367–2374, May 2012.

IV J. Markkanen P. Ylä-Oijala, and A. Sihvola. Discretization of volume integral equation formulations for extremely anisotropic materials. *IEEE Transactions on Antennas and Propagation*, vol. 60, no. 11, pp. 5195–5202, November 2012.

V I. V. Lindell, J. Markkanen, A. Sihvola, and P. Ylä-Oijala. Realization of spherical D′B′ boundary by a layer of wave-guiding medium. *Metamaterials*, vol. 5, no. 4, pp. 149-154, December 2011.

VI S. Järvenpää, J. Markkanen, and P. Ylä-Oijala. Broadband multilevel fast multipole algorithm for electric-magnetic current volume integral equation. Accepted for publication in *IEEE Transactions on Antennas and Propagation*, May 2013.

Author's Contribution

Publication I: "Computation of scattering by DB objects with surface integral equation method"

The first paper is based on the author's Master's thesis. The idea to study electromagnetic properties of the DB boundary by using a surface integral equation method came from Prof. Sihvola and Dr. Ylä-Oijala. The computer codes and calculations were provided by the author. The text was written in collaboration.

Publication II: "Surface integral equation method for scattering by DB objects with sharp wedges"

This paper is an extended version of a conference presentation by the author. The idea arose in collaboration. The quasistatic and numerical analysis for fields near the DB wedge were performed by the author. The text was mainly written by the author while Prof. Sihvola and Dr. Ylä-Oijala gave helpful comments and suggestions.

Publication III: "Analysis of volume integral equation formulations for scattering by high-contrast penetrable objects"

The author implemented most of the codes and performed the analysis. Prof. Lu and Dr. Cao provided results computed by the D-formulation. The manuscript was prepared by Dr. Ylä-Oijala and the author while Prof. Lu and Dr. Cao helped improving the manuscript with comments.

Publication IV: "Discretization of volume integral equation formulations for extremely anisotropic materials"

The author wrote the manuscript, implemented most of the computer codes, and computed the results. The co-authors helped to choose some numerical examples and provided useful comments and suggestions on the manuscript.

Publication V: "Realization of spherical D′B′ boundary by a layer of wave-guiding medium"

This paper is mainly made by Prof. emeritus I. V. Lindell. The author provided numerical codes and computations.

Publication VI: "Broadband multilevel fast multipole algorithm for electric-magnetic current volume integral equation"

Dr. Järvenpää implemented the fast solver for the formulation derived in Publication IV. The author computed the results and helped to prepare the manuscript.

List of abbreviations

BEM	Boundary element method
CFIE	Combined field integral equation
DB	DB boundary condition
D′B′	D′B′ boundary condition
EFIE	Electric field integral equation
GMRES	Generalized minimal residual method
MFIE	Magnetic field integral equation
MLFMA	Multilevel fast multipole algorithm
PEC	Perfect electric conductor
PEMC	Perfect electromagnetic conductor
PMC	Perfect magnetic conductor
RWG	Rao-Wilton-Glisson basis function
SIE	Surface integral equation
SWG	Schaubert–Wilton–Glisson basis function
TEM	Transverse electromagnetic
VIE	Volume integral equation

List of symbols

$\boldsymbol{b}$	Microscopic magnetic flux density
$\boldsymbol{B}$	Macroscopic magnetic flux density
D	Three dimensional domain
$\boldsymbol{D}$	Macroscopic electric flux density
$\boldsymbol{e}$	Microscopic electric field
$\boldsymbol{E}$	Macroscopic electric field
$\boldsymbol{E}^{inc}$	Incident electric field
$\boldsymbol{E}^{s}$	Scattered electric field
f	Frequency
$\boldsymbol{F}$	Force
G	Green's function
$\boldsymbol{H}$	Macroscopic magnetic field
$\boldsymbol{H}^{inc}$	Incident magnetic field
$\boldsymbol{H}^{s}$	Scattered magnetic field
i	Imaginary unit
$\bar{\bar{I}}$	Identity dyadic
$\boldsymbol{j}_b$	Microscopic bound current density
$\boldsymbol{J}_B$	Macroscopic bound current density
$\boldsymbol{J}_c$	Conductivity current density
$\boldsymbol{j}_f$	Microscopic free current density
$\boldsymbol{J}_F$	Macroscopic free current density
$\boldsymbol{J}_s$	Electric surface current density
$\boldsymbol{J}_S$	Equivalent electric surface current density
$\boldsymbol{j}_{tot}$	Microscopic current density
$\boldsymbol{J}_{TOT}$	Macroscopic current density
$\boldsymbol{J}_V$	Equivalent electric volume current density
k	Wave number
$\boldsymbol{k}$	Wave vector

M	PEMC admittance parameter
$\boldsymbol{M}$	Magnetization
$\boldsymbol{M}_S$	Equivalent magnetic surface current density
$\boldsymbol{M}_V$	Equivalent magnetic volume current density
$\hat{\boldsymbol{n}}$	Unit normal vector
$\boldsymbol{P}$	Polarization density
q	Point charge
$\boldsymbol{r}$	Observation point
$\boldsymbol{r}'$	Source point
S	Surface in three dimensions
t	Time
$\boldsymbol{u}_x, \boldsymbol{u}_y, \boldsymbol{u}_x$	Unit vectors of cartesian coodinate system
$\boldsymbol{u}_r, \boldsymbol{u}_\phi, \boldsymbol{u}_\theta$	Unit vectors of spherical coodinate system
$\boldsymbol{v}$	Velocity vector
V	Volume
$\bar{\bar{Z}}_S$	Surface impedance dyadic
$\bar{\bar{\alpha}}$	Material parameter dyadic
$\bar{\bar{\beta}}$	Material parameter dyadic
δ	Kronecker's delta function
ϵ_0	Vacuum permittivity
ϵ	Isotropic permittivity
ϵ_r	Isotropic relavite permittivity
ϵ_r^r	Radial component of relative permittivity
ϵ_r^t	Transverse component of relative permittivity
$\bar{\bar{\epsilon}}$	Electric permittivity dyadic
$\bar{\bar{\epsilon}}_r$	Relative electric permittivity dyadic
$\bar{\bar{\epsilon}}'$	Material parameter dyadic
$\bar{\bar{\zeta}}$	Magnetoelectric response dyadic
$\bar{\bar{\zeta}}_r$	Relative magnetoelectric response dyadic
η	Wave impedance
λ	Wavelength
μ_0	Vacuum permeability
μ	Isotropic permeability
μ_r	Isotropic relative permeability
μ_r^r	Radial component of relative permeability
μ_r^t	Transverse component of relative permeability

$\bar{\bar{\mu}}$	Magnetic permeability dyadic
$\bar{\bar{\mu}}_r$	Relative magnetic permeability dyadic
$\bar{\bar{\xi}}$	Magnetoelectric response dyadic
$\bar{\bar{\xi}}_r$	Relative magnetoelectric response dyadic
ρ_b	Microscopic bound charge density
ρ_B	Macroscopic bound charge density
ρ_f	Microscopic free charge density
ρ_F	Macroscopic free charge density
ρ_s	Surface charge density
ρ_{tot}	Microscopic charge density
ρ_{TOT}	Macroscopic charge density
$\bar{\bar{\sigma}}$	Conductivity dyadic
ω	Angular frequency
Ω	Domain
Ω_s	Solid angle

1. Introduction

In classical electromagnetic field theory, the behavior of electromagnetic fields can be described by a set of partial differential equations known as Maxwell's equations. Maxwell's equations are based on early observations by Gauss, Faraday, and Ampère in the 19th century. These empirical laws were completed and combined by James Clerk Maxwell and published individually in the four-part paper *On Physical Lines of Force* [1] between 1861 and 1862. In 1865, Maxwell showed that this new theory allowed the electric and magnetic fields to propagate across empty space as an electromagnetic wave and concluded that visible light is a part of electromagnetic radiation [2].

A fundamental problem in electromagnetics is to solve scattered fields from obstacles when the incident fields are known. Such a problem is called a scattering problem. Properties of these obstacles can be described by the following material parameters: the permittivity $\bar{\bar{\epsilon}}$, permeability $\bar{\bar{\mu}}$, and magnetoelectric parameters $\bar{\bar{\xi}}$ and $\bar{\bar{\zeta}}$, which, in a general case, can be complicated functions of position, frequency, direction, and strength of the fields. In order to solve Maxwell's equations in a medium, which contains material objects described by material parameters, the equations have to be solved both in the background medium and inside the objects such that the continuity conditions of the fields are satisfied. A scattering problem can also be formulated as a boundary value problem for Maxwell's equations. In this approach, the scatterer is removed, and the field quantities are forced to satisfy given conditions at the boundary, known as *boundary conditions*. Boundary conditions are purely mathematical, and they should not be confused with the physical conditions for fields across material interfaces. Nevertheless, they can be useful as approximations of real material interfaces since they simplify the analysis. On the other hand, boundary conditions might have some interesting properties for en-

gineering purposes, and therefore, finding a real material interface that approximates the boundary condition is of great interest.

Recently introduced boundary conditions known as DB and D′B′ boundary conditions have been found to have some intriguing electromagnetic properties, for example, zero backscattering [3, 4]. Moreover, the DB boundary acts as an electromagnetic soft surface and the D′B′ as a hard surface in the definition of Kildal [5, 6] i.e., electromagnetic power cannot propagate (soft) or has a maximum (hard) along the surface. The converses are not necessarily true. The DB boundary requires that the electric and magnetic flux densities $\boldsymbol{D}$ and $\boldsymbol{B}$ normal to the boundary vanish [7]. At the D′B′ boundary, the normal derivatives of the normal components of the flux densities tend to zero [4]. In nature, there are no materials that mimic these nonconventional boundaries. However, in the field of metamaterials i.e., artificially engineered materials (see, for example [8, 9]), the fabrication of such material interfaces might be possible. Therefore, these boundaries could give rise to new electromagnetic engineering applications [10]. Particularly, the property of being either a soft or hard surface finds many micro- and millimeter wave applications, for example, improving polarization, narrowing beams, reducing side lobes of antennas, miniaturizing waveguides, etc. [7, 11, 12]. In addition, the DB boundary condition has proved to be relevant in the cloaking of objects from electromagnetic radiation [13, 14, 15, 16].

To obtain a better understanding about electromagnetic field interaction with complicated materials and surfaces, a solution for Maxwell's equations needs to be found. However, finding a solution for Maxwell's equations is not easy. In 1908, Gustav Mie was able to find an analytical solution for the electromagnetic wave scattering by spherical obstacles [17]. Yet analytical solutions can be found only for very simple problems, and therefore, to solve Maxwell's equations in cases of practical interests such as antenna design, radar applications, medical imaging, and material modeling, sophisticated numerical methods are needed.

Numerical methods for solving Maxwell's equations can be formulated as either differential equations for field functions or integral equations for source functions. The integral equations are well suited for unbounded problems such as scattering problems since the source function lives inside or on the surface of the scatterer, and therefore, only the scatterer needs to be modeled. In the differential equation methods, however, the field function is global, and the whole space has to be modeled. In practice,

it means that the computational domain must be terminated by some absorbing boundary condition or a perfectly matched layer. In a numerical point of view, numerical differentiation is more difficult than numerical integration due to the fact that differentiation decreases the regularity of a function, and thus, numerical methods based on integral equations are, in general, more accurate and stable. However, integral equation methods lead to full matrix systems and thus higher computational costs than differential equation methods, which give rise to sparse matrices. Fortunately, the computational costs of integral equation methods can be decreased by applying sophisticated fast algorithms.

The main objective of this thesis is to develop numerical methods based on integral equations for analyzing electromagnetic scattering properties of objects with extraordinary boundary conditions and materials with complicated responses. The thesis consists of an overview and six peer-reviewed journal articles. In Publications I and II, the surface integral equation (SIE) solution for the DB boundary is presented, and the electromagnetic properties of the ideal DB objects are analyzed. In addition, the accuracy and stability of the surface integral equation method–based solution for arbitrarily shaped DB objects is investigated. The material approximations of boundaries such as DB and D′B′ may require media with extreme material parameters, which can cause problems for conventional numerical schemes. Different discretizations of volume integral equations (VIEs) for high-contrast objects are investigated in Publication III, and a stable discretization of the VIE for highly anisotropic media is introduced in Publication IV. The method is also applied for the approximations of the DB and D′B′ objects in Publications IV and V, respectively. Furthermore, in Publication VI, the multilevel fast multipole algorithm (MLFMA) is used for accelerating VIE solution, and the method is applied to the cloaking structure.

2. Electromagnetics

Electromagnetism is the force that interacts between electrically charged particles and is one of four fundamental force interactions in nature among the strong and weak interactions and gravitation. The electromagnetic theory is formulated as a field theory in which electromagnetism manifests itself as electric and magnetic fields. In this chapter, the basic theory of the classical electromagnetics is introduced. In addition, material interaction with the electromagnetic field is discussed.

2.1 Microscopic Maxwell's equations

In classical electromagnetic field theory, a complete description of the behavior of electromagnetic fields can be written as a set of four partial differential equations known as the microscopic Maxwell's equations [18]:

$$\nabla \times \boldsymbol{e}(\boldsymbol{r},t) = -\frac{\partial \boldsymbol{b}(\boldsymbol{r},t)}{\partial t}, \tag{2.1}$$

$$\nabla \times \boldsymbol{b}(\boldsymbol{r},t) = \mu_0 \boldsymbol{j}_{tot}(\boldsymbol{r},t) + \mu_0 \epsilon_0 \frac{\partial \boldsymbol{e}(\boldsymbol{r},t)}{\partial t}, \tag{2.2}$$

$$\nabla \cdot \boldsymbol{e}(\boldsymbol{r},t) = \frac{\rho_{tot}(\boldsymbol{r},t)}{\epsilon_0}, \tag{2.3}$$

$$\nabla \cdot \boldsymbol{b}(\boldsymbol{r},t) = 0, \tag{2.4}$$

where $\boldsymbol{e}$ (measured in V/m) is the electric field and $\boldsymbol{b}$ (Vs/m^2) is the magnetic flux density. The electric permittivity and magnetic permeability of vacuum are denoted by ϵ_0 (As/Vm) and μ_0 (Vs/Am), respectively. Maxwell's equations together with the Lorentz force interaction form a complete theory of the electromagnetic field. The Lorentz force is the force acting on a point charge due to the electric and magnetic fields given by

$$\boldsymbol{F}(\boldsymbol{r},t) = q[\boldsymbol{e}(\boldsymbol{r},t) + \boldsymbol{v} \times \boldsymbol{b}(\boldsymbol{r},t)], \tag{2.5}$$

where q is a charge and $\boldsymbol{v}$ is the velocity of the charged particle q.

Sources of the fields are described by the total electric charge density ρ_{tot} (As/m^3) as

$$\rho_{tot}(\boldsymbol{r},t) = \sum_{n=1}^{N} q_n \delta(\boldsymbol{r} - \boldsymbol{r}') \tag{2.6}$$

and the total electric current density $\boldsymbol{j}_{tot}$ (A/m^2)

$$\boldsymbol{j}_{tot}(\boldsymbol{r},t) = \sum_{n=1}^{N} q_n \boldsymbol{v}_n \delta(\boldsymbol{r} - \boldsymbol{r}'), \tag{2.7}$$

where δ is Kronecker's delta function and $\boldsymbol{v}_n$ is the velocity related to the point charge q_n. The sources obey the equation of continuity:

$$\nabla \cdot \boldsymbol{j}_{tot}(\boldsymbol{r},t) = -\frac{\partial \rho_{tot}(\boldsymbol{r},t)}{\partial t}, \tag{2.8}$$

which is a direct consequence of equations (2.2) and (2.3). The equation of continuity states that the charge is conserved which is more fundamental principle than Maxwell's equations.

2.2 Material interaction and macroscopic Maxwell's equations

Since charged particles are sources for electromagnetic fields, it is obvious that materials, which are complicated structures of charged particles (e.g., atoms, molecules, etc.), affect the behavior of electromagnetic fields [19]. To obtain Maxwell's equations in matter, also known as the macroscopic Maxwell's equations [18], the sources are separated into bound and free parts as

$$\begin{aligned} \boldsymbol{j}_{tot}(\boldsymbol{r},t) &= \boldsymbol{j}_b(\boldsymbol{r},t) + \boldsymbol{j}_f(\boldsymbol{r},t), \\ \rho_{tot}(\boldsymbol{r},t) &= \rho_b(\boldsymbol{r},t) + \rho_f(\boldsymbol{r},t), \end{aligned} \tag{2.9}$$

and averaged over some suitable volume and time

$$\begin{aligned} \boldsymbol{J}_{TOT}(\boldsymbol{r},t) &= \boldsymbol{J}_B(\boldsymbol{r},t) + \boldsymbol{J}_F(\boldsymbol{r},t) = \langle \boldsymbol{j}_b(\boldsymbol{r},t) \rangle_{V,T} + \langle \boldsymbol{j}_f(\boldsymbol{r},t) \rangle_{V,T}, \\ \rho_{TOT}(\boldsymbol{r},t) &= \rho_B(\boldsymbol{r},t) + \rho_F(\boldsymbol{r},t) = \langle \rho_b(\boldsymbol{r},t) \rangle_{V,T} + \langle \rho_f(\boldsymbol{r},t) \rangle_{V,T}, \end{aligned} \tag{2.10}$$

where average is taken over space-time as

$$\langle f(\boldsymbol{r},t) \rangle_{V,T} = \frac{1}{VT} \int_V \int_{-T/2}^{T/2} f(\boldsymbol{r}+\boldsymbol{r}', t-t') \, \mathrm{d}t' \, \mathrm{d}\boldsymbol{r}'. \tag{2.11}$$

The bound charge and current densities can be written in terms of an average polarization $\boldsymbol{P}$ and magnetization $\boldsymbol{M}$ by

$$\rho_B(\boldsymbol{r},t) = -\nabla \cdot \boldsymbol{P}(\boldsymbol{r}, \boldsymbol{E}, \boldsymbol{B}), \tag{2.12}$$

and

$$\boldsymbol{J}_B(\boldsymbol{r},t) = \frac{\partial \boldsymbol{P}(\boldsymbol{r},\boldsymbol{E},\boldsymbol{B})}{\partial t} + \nabla \times \boldsymbol{M}(\boldsymbol{r},\boldsymbol{B},\boldsymbol{E}), \tag{2.13}$$

where $\boldsymbol{E}$ and $\boldsymbol{B}$ denote the average electric $\langle \boldsymbol{e} \rangle$ and magnetic $\langle \boldsymbol{b} \rangle$ fields, respectively. The polarization is caused by bound charges when the electric or magnetic fields are applied. This is because they cannot move freely but only shift from their average equilibrium positions. The magnetization emerges from the angular momenta of elementary particles or microscopic currents.

By defining auxiliary fields $\boldsymbol{D}$ (measured in As/m^2) and $\boldsymbol{H}$ (A/m) in terms of the polarization $\boldsymbol{P}$ and magnetization $\boldsymbol{M}$ as

$$\boldsymbol{D}(\boldsymbol{r},t) = \epsilon_0 \boldsymbol{E}(\boldsymbol{r},t) + \boldsymbol{P}(\boldsymbol{r},\boldsymbol{E},\boldsymbol{B}), \tag{2.14}$$

$$\boldsymbol{H}(\boldsymbol{r},t) = \mu_0^{-1} \boldsymbol{B}(\boldsymbol{r},t) - \boldsymbol{M}(\boldsymbol{r},\boldsymbol{B},\boldsymbol{E}), \tag{2.15}$$

the contributions of the bound currents $\boldsymbol{J}_B$ and charges ρ_B can be included in them. In a general medium, the auxiliary fields can be expressed in terms of the four material parameter dyadics $\overline{\overline{\epsilon}}'$, $\overline{\overline{\mu}}$, $\overline{\overline{\alpha}}$, and $\overline{\overline{\beta}}$ as convolutions:

$$\begin{aligned} \boldsymbol{D}(\boldsymbol{r},t) = &\int_{-\infty}^{t} \int_{V'} \overline{\overline{\epsilon}}'(\boldsymbol{r}+\boldsymbol{r}', t-t'; \boldsymbol{E}) \cdot \boldsymbol{E}(\boldsymbol{r}',t') \, \mathrm{d}r' \mathrm{d}t' \\ &+ \int_{-\infty}^{t} \int_{V'} \overline{\overline{\alpha}}(\boldsymbol{r}+\boldsymbol{r}', t-t'; \boldsymbol{B}) \cdot \boldsymbol{B}(\boldsymbol{r}',t') \, \mathrm{d}r' \mathrm{d}t', \end{aligned} \tag{2.16}$$

$$\begin{aligned} \boldsymbol{H}(\boldsymbol{r},t) = &\int_{-\infty}^{t} \int_{V'} \overline{\overline{\mu}}^{-1}(\boldsymbol{r}+\boldsymbol{r}', t-t'; \boldsymbol{B}) \cdot \boldsymbol{B}(\boldsymbol{r}',t') \, \mathrm{d}r' \mathrm{d}t' \\ &+ \int_{-\infty}^{t} \int_{V'} \overline{\overline{\beta}}(\boldsymbol{r}+\boldsymbol{r}', t-t'; \boldsymbol{E}) \cdot \boldsymbol{E}(\boldsymbol{r}',t') \, \mathrm{d}r' \mathrm{d}t'. \end{aligned} \tag{2.17}$$

The above relations are known as constitutive relations. In electromagnetic theory, the flux densities $(\boldsymbol{D}, \boldsymbol{B})$ and fields $(\boldsymbol{E}, \boldsymbol{H})$ are often considered as pairs, and the constitutive relations are expressed as follows:

$$\begin{aligned} \boldsymbol{D}(\boldsymbol{r},t) = &\int_{-\infty}^{t} \int_{V'} \overline{\overline{\epsilon}}(\boldsymbol{r}+\boldsymbol{r}', t-t'; \boldsymbol{E}) \cdot \boldsymbol{E}(\boldsymbol{r}',t') \, \mathrm{d}r' \mathrm{d}t' \\ &+ \int_{-\infty}^{t} \int_{V'} \overline{\overline{\xi}}(\boldsymbol{r}+\boldsymbol{r}', t-t'; \boldsymbol{H}) \cdot \boldsymbol{H}(\boldsymbol{r}',t') \, \mathrm{d}r' \mathrm{d}t', \end{aligned} \tag{2.18}$$

$$\begin{aligned} \boldsymbol{B}(\boldsymbol{r},t) = &\int_{-\infty}^{t} \int_{V'} \overline{\overline{\mu}}(\boldsymbol{r}+\boldsymbol{r}', t-t'; \boldsymbol{H}) \cdot \boldsymbol{H}(\boldsymbol{r}',t') \, \mathrm{d}r' \mathrm{d}t' \\ &+ \int_{-\infty}^{t} \int_{V'} \overline{\overline{\zeta}}(\boldsymbol{r}+\boldsymbol{r}', t-t'; \boldsymbol{E}) \cdot \boldsymbol{E}(\boldsymbol{r}',t') \, \mathrm{d}r' \mathrm{d}t', \end{aligned} \tag{2.19}$$

where $\bar{\bar{\epsilon}}$ is the electric permittivity, $\bar{\bar{\mu}}$ is the magnetic permeability, and $\bar{\bar{\xi}}$ and $\bar{\bar{\zeta}}$ are the magnetoelectric parameters.

Finally, by using the averaged physical and auxiliary fields, the macroscopic Maxwell's equations can be written as

$$\nabla \times \boldsymbol{E}(\boldsymbol{r},t) = -\frac{\partial \boldsymbol{B}(\boldsymbol{r},t)}{\partial t}, \tag{2.20}$$

$$\nabla \times \boldsymbol{H}(\boldsymbol{r},t) = \boldsymbol{J}_F(\boldsymbol{r},t) + \frac{\partial \boldsymbol{D}(\boldsymbol{r},t)}{\partial t}, \tag{2.21}$$

$$\nabla \cdot \boldsymbol{D}(\boldsymbol{r},t) = \rho_F(\boldsymbol{r},t), \tag{2.22}$$

$$\nabla \cdot \boldsymbol{B}(\boldsymbol{r},t) = 0, \tag{2.23}$$

in which the material interactions are embedded in the auxiliary fields via constitutive relations.

Using the macroscopic Maxwell's equations allows an analysis of field behavior inside the matter on average, meaning that some microscopic details may have been lost. A detailed derivation of the macroscopic Maxwell's equations can be found in [18].

2.3 Time-harmonic equations

Often, it can be convenient to analyze electromagnetic problems in the frequency domain—that is, the time dependency is assumed to be of the form $exp(-i\omega t)$, where ω is the angular frequency. Now the field is described by a complex-valued function $\boldsymbol{F}(\boldsymbol{r})$, and a conversion back to time domain is obtained as follows:

$$\boldsymbol{F}(\boldsymbol{r},t) = Re\{\boldsymbol{F}(\boldsymbol{r})e^{-i\omega t}\}. \tag{2.24}$$

Suppressing the time dependence, the time-harmonic Maxwell's equations can be written as

$$\nabla \times \boldsymbol{E}(\boldsymbol{r}) = i\omega \boldsymbol{B}(\boldsymbol{r}), \tag{2.25}$$

$$\nabla \times \boldsymbol{H}(\boldsymbol{r}) = \boldsymbol{J}_F(\boldsymbol{r}) - i\omega \boldsymbol{D}(\boldsymbol{r}), \tag{2.26}$$

$$\nabla \cdot \boldsymbol{D}(\boldsymbol{r}) = \rho_F(\boldsymbol{r}), \tag{2.27}$$

$$\nabla \cdot \boldsymbol{B}(\boldsymbol{r}) = 0, \tag{2.28}$$

and the constitutive relations in linear medium read as

$$\boldsymbol{D}(\boldsymbol{r}) = \bar{\bar{\epsilon}}(\boldsymbol{r}) \cdot \boldsymbol{E}(\boldsymbol{r}) + \bar{\bar{\xi}}(\boldsymbol{r}) \cdot \boldsymbol{H}(\boldsymbol{r}), \tag{2.29}$$

$$\boldsymbol{B}(\boldsymbol{r}) = \bar{\bar{\mu}}(\boldsymbol{r}) \cdot \boldsymbol{H}(\boldsymbol{r}) + \bar{\bar{\zeta}}(\boldsymbol{r}) \cdot \boldsymbol{E}(\boldsymbol{r}). \tag{2.30}$$

The advantage of using the time-harmonic Maxwell's equations is that the time derivatives are replaced by algebraic multiplications of $-i\omega$. In addition, the constitutive relations in the frequency domain are multiplications, whereas in the time domain, they are convolutions.

The response of the conductivity current $\boldsymbol{J}_c = \bar{\bar{\sigma}} \cdot \boldsymbol{E}$ can also be included in $\boldsymbol{D}$ by adding the imaginary part to the material parameter since

$$\begin{aligned} \nabla \times \boldsymbol{H}(\boldsymbol{r}) &= \boldsymbol{J}_c(\boldsymbol{r}) - i\omega \boldsymbol{D}(\boldsymbol{r}) = \bar{\bar{\sigma}}(\boldsymbol{r}) \cdot \boldsymbol{E}(\boldsymbol{r}) - i\omega \bar{\bar{\epsilon}}(\boldsymbol{r}) \cdot \boldsymbol{E}(\boldsymbol{r}) \\ &= -i\omega \left(\bar{\bar{\epsilon}}(\boldsymbol{r}) + i \frac{\bar{\bar{\sigma}}(\boldsymbol{r})}{\omega} \right) \cdot \boldsymbol{E}(\boldsymbol{r}) = -i\omega \bar{\bar{\epsilon}}_c(\boldsymbol{r}) \cdot \boldsymbol{E}(\boldsymbol{r}), \end{aligned} \tag{2.31}$$

in which the complex permittivity is given by

$$\bar{\bar{\epsilon}}_c(\boldsymbol{r}) = \bar{\bar{\epsilon}}(\boldsymbol{r}) + i \frac{\bar{\bar{\sigma}}(\boldsymbol{r})}{\omega}, \tag{2.32}$$

and $\bar{\bar{\sigma}}(\boldsymbol{r})$ is the conductivity. However, it is important to understand that the real part and imaginary part of the complex permittivity are not completely independent. Behaviors of these as functions of frequency are restricted by Kramers-Kronig relations, which arise from causality [20].

In the rest of this thesis, the time dependence $exp(-i\omega t)$ is assumed and suppressed, and the complex permittivity is denoted by $\bar{\bar{\epsilon}}$.

2.4 Interface and boundary conditions

Consider an interface between the two electromagnetic media D_1 and D_2, where $\hat{\boldsymbol{n}}$ is the unit normal vector of the interface as shown in Fig. 2.1. The material parameters in D_1 are $\bar{\bar{\epsilon}}_1$ and $\bar{\bar{\mu}}_1$, and in D_2, they are $\bar{\bar{\epsilon}}_2$ and $\bar{\bar{\mu}}_2$. The fields satisfy Maxwell's equations in both domains, and at the interface, they satisfy the interface conditions given by

$$\hat{\boldsymbol{n}} \times (\boldsymbol{E}_2 - \boldsymbol{E}_1) = 0, \tag{2.33}$$

$$\hat{\boldsymbol{n}} \times (\boldsymbol{H}_2 - \boldsymbol{H}_1) = \boldsymbol{J}_s, \tag{2.34}$$

$$\hat{\boldsymbol{n}} \cdot (\boldsymbol{D}_2 - \boldsymbol{D}_1) = \rho_s, \tag{2.35}$$

$$\hat{\boldsymbol{n}} \cdot (\boldsymbol{B}_2 - \boldsymbol{B}_1) = 0, \tag{2.36}$$

where $\boldsymbol{J}_s$ and ρ_s denote the surface current and charge densities, respectively.

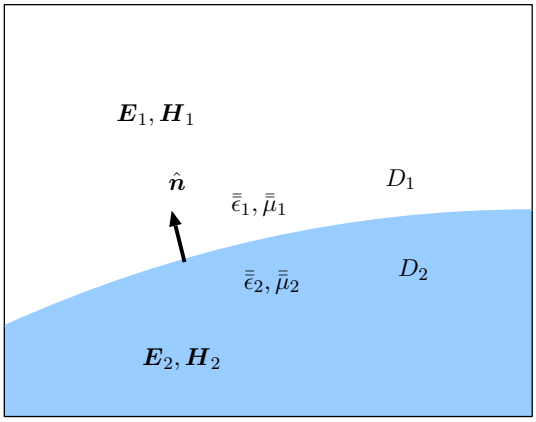

Figure 2.1. Material interface between two electromagnetic media.

It is important to note that interfaces and boundaries are fundamentally different concepts. The fields interact with each other across the interfaces through interface conditions (2.33)–(2.36), whereas a boundary terminates the region of interest by imposing a mathematical condition known as a boundary condition. Hence, nothing behind the boundary can affect the other side.

In electromagnetics, the most commonly used boundary condition is a perfect electric conductor (PEC) boundary condition [21]. It is a good approximation for highly conducting surfaces, such as silver or copper, at low frequencies (e.g., microwave frequencies or lower). It states that the tangential component of the electric field vanishes on the boundary

$$\boldsymbol{E}_{tan} = 0. \tag{2.37}$$

Analogously, a perfect magnetic conductor (PMC) boundary condition can be defined as

$$\boldsymbol{H}_{tan} = 0. \tag{2.38}$$

The PEC and PMC boundary conditions are special cases of a more general impedance boundary condition (IBC) [22, 23]

$$\boldsymbol{E}_{tan} = \bar{\bar{\boldsymbol{Z}}}_S \cdot \hat{\boldsymbol{n}} \times \boldsymbol{H}, \tag{2.39}$$

in which $\bar{\bar{Z}}_S$ denotes the surface impedance, or a perfect electromagnetic conductor (PEMC) boundary condition [24]

$$\hat{\boldsymbol{n}} \times \boldsymbol{H} = M \hat{\boldsymbol{n}} \times \boldsymbol{E}, \tag{2.40}$$

where M is an admittance-type parameter.

Instead of restricting the freedom of the tangential components of the fields like in the above cases, we can also require conditions for normal components of the fields at the surface. The DB boundary condition [7], originally introduced in [25], requires that the normal components of the electric and magnetic flux densities $\boldsymbol{D}, \boldsymbol{B}$ vanish on the surface:

$$\hat{\boldsymbol{n}} \cdot \boldsymbol{D} = 0, \quad \hat{\boldsymbol{n}} \cdot \boldsymbol{B} = 0. \tag{2.41}$$

The existence and uniqueness theorems for the solution involving the DB boundary condition were introduced by Yee [26] for simply connected domains and by Kress [27] for multiply connected domains. In the latter case, some additional conditions have to be required.

A boundary condition for the derivatives of the flux densities

$$\nabla \cdot (\hat{\boldsymbol{n}}\hat{\boldsymbol{n}} \cdot \boldsymbol{D}) = 0, \quad \nabla \cdot (\hat{\boldsymbol{n}}\hat{\boldsymbol{n}} \cdot \boldsymbol{B}) = 0, \tag{2.42}$$

was introduced, and dubbed as a D′B′ boundary condition in [4]. On planar surfaces, it states that the normal derivatives of the normal components of the flux densities are zero:

$$\frac{\partial}{\partial n}\hat{\boldsymbol{n}} \cdot \boldsymbol{D} = 0, \quad \frac{\partial}{\partial n}\hat{\boldsymbol{n}} \cdot \boldsymbol{B} = 0. \tag{2.43}$$

However, the existence and uniqueness of the solution is still an open problem for the D′B′ boundary condition.

3. Method of moments

Method of moments (MoM) [28] is a projection method to solve linear problems of the form

$$Lu = f, \tag{3.1}$$

where $L : U \to F$ is a linear operator from a Hilbert space U to another Hilbert space F with the given function $f \in F$ and the unknown function $u \in U$. Let us denote the inner product on F as $\langle f, g \rangle_F$ with $f, g \in F$.

The first step is to approximate the unknown function u by expanding it as a linear combination of so-called basis functions b_n, which spans a finite dimensional subspace $B_N \subset U$ as

$$u \approx \tilde{u}_N = \sum_{n=1}^{N} c_n b_n, \tag{3.2}$$

where c_n are the unknown coefficients.

Next, the residual

$$R_N = L\tilde{u}_N - f, \tag{3.3}$$

is minimized by requiring it to be orthogonal to a finite dimensional subspace $T_M \subset F$. The space T_M is spanned by testing functions t_m. Therefore, by using orthogonality requirement

$$\langle t_m, R_N \rangle_F = 0, \;\; m = 1, ..., M, \tag{3.4}$$

we obtain

$$\sum_{n=1}^{N} c_n \langle t_m, Lb_n \rangle_F = \langle t_m, f \rangle_F, \;\; \text{for all} \;\; m = 1, ..., M, \tag{3.5}$$

from which the unknown coefficients can be solved. In matrix form, equation (3.5) reads

$$\boldsymbol{A}\boldsymbol{x} = \boldsymbol{b}, \tag{3.6}$$

where

$$A_{mn} = \langle t_m, Lb_n \rangle_F, \tag{3.7}$$

$$x_n = c_n, \tag{3.8}$$

$$b_m = \langle t_m, f \rangle_F. \tag{3.9}$$

3.1 Choice of basis and testing functions

The accuracy of the numerical solution with MoM strongly depends on an underlying integral equation as well as a choice of basis and testing functions. Choosing a proper set of basis functions is relatively easy. The basis functions should be able to represent the physical properties of the unknown under approximation. In other words, they should span the domain of the integral operator. These physical properties of the unknowns come from Maxwell's equations and the finite energy assumption. For the fields and flux densities, they read as [29]

$$\boldsymbol{E}, \boldsymbol{H} \in \mathcal{H}_{curl}(\Omega) = \{\boldsymbol{u} \in L^2(\Omega);\ \ \nabla \times \boldsymbol{u} \in L^2(\Omega)\}, \tag{3.10}$$

$$\boldsymbol{D}, \boldsymbol{B} \in \mathcal{H}_{div}(\Omega) = \{\boldsymbol{u} \in L^2(\Omega);\ \ \nabla \cdot \boldsymbol{u} \in L^2(\Omega)\}, \tag{3.11}$$

respectively, in which $L^2(\Omega)$ is a function space of square integrable functions in Ω. From the definitions of equivalent volumetric polarization currents $\boldsymbol{J}_V = -i\omega\epsilon_0(\bar{\bar{\epsilon}}_r - \bar{\bar{I}})$ and $\boldsymbol{M}_V = -i\omega\mu_0(\bar{\bar{\mu}}_r - \bar{\bar{I}})$, it is easy to see that they are not continuous across material interfaces. Hence, the finite energy space for the polarization currents reads as [30]

$$\boldsymbol{J}_V, \boldsymbol{M}_V \in L^2(\Omega). \tag{3.12}$$

The proper function spaces for the surface equivalent currents and tangential traces of the fields are given by

$$\boldsymbol{J}_S, \boldsymbol{M}_S \in \mathcal{H}_{div}^{-1/2}(S) = \{\boldsymbol{u} \in \mathcal{H}^{-1/2}(S);\ \ \nabla_s \cdot \boldsymbol{u} \in \mathcal{H}^{-1/2}(S)\}, \tag{3.13}$$

$$\boldsymbol{E}_S, \boldsymbol{H}_S \in \mathcal{H}_{curl}^{-1/2}(S) = \{\boldsymbol{u} \in \mathcal{H}^{-1/2}(S);\ \ \hat{\boldsymbol{n}} \cdot \nabla_s \times \boldsymbol{u} \in \mathcal{H}^{-1/2}(S)\}, \tag{3.14}$$

where $\mathcal{H}^{-1/2}(S)$ denotes the standard fractional order Sobolev space defined on the surface S [31].

The choice of the testing functions is not as obvious as the choice of the basis functions. If the testing functions are the same functions as the basis functions, the scheme is called Galerkin's method, and it has been the most popular method for discretizing integral equations [32]. However, Galerkin's method does not always lead to an accurate and stable solution, especially when the L^2 inner product is employed. It is suggested

that to obtain convergence in the norm of the solution, the testing functions should span the L^2 dual space of the range of the operator [30, 33]. In this case, basis and testing functions do not necessarily have to be the same functions, but they have to be paired properly. Hence, it is essential to know mapping properties of the linear operator before choosing testing functions.

For example, it is well-known that the solution accuracy is poor when Galerkin's method is applied for the surface magnetic field integral equation (MFIE) [34]. In [35], it was theoretically proven and numerically demonstrated that by testing the MFIE in the dual space of the range, the solution converges and is more accurate than the Galerkin tested one. Similar observations were made for other surface integral equations in [36].

4. Surface integral equations

A surface integral equation method, also known as a boundary element method (BEM), is an effective numerical scheme for analyzing scattering problems involving objects with boundary conditions or homogeneous objects. The major advantage is that only the surface of the object has to be discretized, which reduces computational costs. In this section, the basic formulations are introduced, and how to enforce the DB boundary condition is shown.

4.1 Surface equivalence principle

Consider an arbitrarily shaped three-dimensional object D_1 in a homogeneous background medium D_2, and incident time-harmonic electromagnetic fields $\boldsymbol{E}^{inc}$ and $\boldsymbol{H}^{inc}$. The surface of the object is denoted by S, and the electromagnetic parameters of the isotropic and homogeneous background medium are ϵ_0 and μ_0.

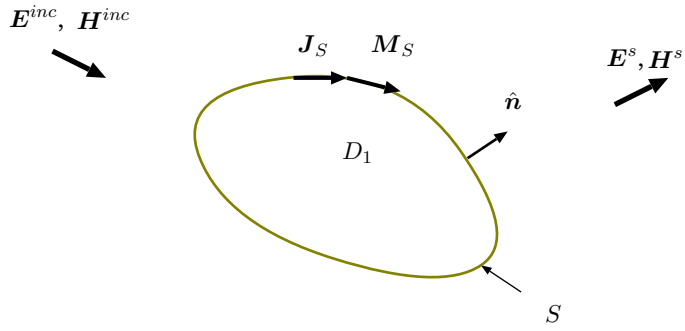

Figure 4.1. In the surface equivalence principle, the scatterer is removed and replaced with the equivalent electric and magnetic surface currents $\boldsymbol{J}_S$ and $\boldsymbol{M}_S$. These equivalent surface currents act as sources for the scattered electric $\boldsymbol{E}^s$ and magnetic fields $\boldsymbol{H}^s$.

Representations for the total time-harmonic electric and magnetic fields

can be written as [37]

$$\begin{aligned}\Omega_s(\boldsymbol{r})\boldsymbol{E}(\boldsymbol{r}) &= \eta\boldsymbol{\mathcal{L}}(\boldsymbol{J}_S)(\boldsymbol{r}) - \boldsymbol{\mathcal{K}}(\boldsymbol{M}_S)(\boldsymbol{r}) + \boldsymbol{E}^{inc}(\boldsymbol{r}),\\ \Omega_s(\boldsymbol{r})\boldsymbol{H}(\boldsymbol{r}) &= \frac{1}{\eta}\boldsymbol{\mathcal{L}}(\boldsymbol{M}_S)(\boldsymbol{r}) + \boldsymbol{\mathcal{K}}(\boldsymbol{J}_S)(\boldsymbol{r}) + \boldsymbol{H}^{inc}(\boldsymbol{r}),\end{aligned} \tag{4.1}$$

where the relative solid angle subtended by the surface

$$\Omega_s(\boldsymbol{r}) = \begin{cases} 1/2, & \boldsymbol{r}\in S\\ 1, & \boldsymbol{r}\in D_1\\ 0, & \boldsymbol{r}\in D_2,\end{cases} \tag{4.2}$$

$\boldsymbol{J}_S = \hat{\boldsymbol{n}}\times\boldsymbol{H}$, and $\boldsymbol{M}_S = -\hat{\boldsymbol{n}}\times\boldsymbol{E}$ are the equivalent electric and magnetic surface current densities, respectively, $\eta = \sqrt{\mu_0/\epsilon_0}$ is the wave impedance, and $\hat{\boldsymbol{n}}$ is the outer unit normal vector of the surface. The surface integral operators are defined as

$$\boldsymbol{\mathcal{L}}(\boldsymbol{F})(\boldsymbol{r}) = -\frac{1}{ik}\nabla\boldsymbol{\mathcal{S}}(\nabla_s'\cdot\boldsymbol{F}) + ik\boldsymbol{\mathcal{S}}(\boldsymbol{F})(\boldsymbol{r}), \tag{4.3}$$

$$\boldsymbol{\mathcal{K}}(\boldsymbol{F})(\boldsymbol{r}) = \nabla\times\boldsymbol{\mathcal{S}}(\boldsymbol{F})(\boldsymbol{r}), \tag{4.4}$$

$$\boldsymbol{\mathcal{S}}(\boldsymbol{F})(\boldsymbol{r}) = \int_S G(\boldsymbol{r},\boldsymbol{r}')\boldsymbol{F}(\boldsymbol{r}')\,\mathrm{d}S(\boldsymbol{r}), \tag{4.5}$$

where G is the Green function

$$G(\boldsymbol{r},\boldsymbol{r}') = \frac{e^{ik|\boldsymbol{r}-\boldsymbol{r}'|}}{4\pi|\boldsymbol{r}-\boldsymbol{r}'|}, \tag{4.6}$$

in which $\boldsymbol{r}$ is the observation point, $\boldsymbol{r}'$ is the source point, and $k = \omega\sqrt{\epsilon\mu}$ is the wave number.

4.2 Surface integral equation formulations

Two alternative formulations can be derived from (4.1). Taking the tangential component of (4.1) and using the definitions of the equivalent surface currents, the T-formulation is obtained:

$$\begin{aligned}\gamma_t\boldsymbol{E}^{inc}(\boldsymbol{r}) &= -\eta\gamma_t\boldsymbol{\mathcal{L}}(\boldsymbol{J}_S)(\boldsymbol{r}) + \gamma_t\boldsymbol{\mathcal{K}}(\boldsymbol{M}_S)(\boldsymbol{r}) + \frac{1}{2}\gamma_r\boldsymbol{M}_S(\boldsymbol{r}),\\ \gamma_t\boldsymbol{H}^{inc}(\boldsymbol{r}) &= -\frac{1}{\eta}\gamma_t\boldsymbol{\mathcal{L}}(\boldsymbol{M}_S)(\boldsymbol{r}) - \gamma_t\boldsymbol{\mathcal{K}}(\boldsymbol{J}_S)(\boldsymbol{r}) - \frac{1}{2}\gamma_r\boldsymbol{J}_S(\boldsymbol{r}),\end{aligned} \tag{4.7}$$

where γ_t takes the tangential trace (on a smooth surface $\gamma_t\boldsymbol{F} = -\hat{\boldsymbol{n}}\times\hat{\boldsymbol{n}}\times\boldsymbol{F}$), and γ_r denotes the rotated tangential trace ($\gamma_r\boldsymbol{F} = \hat{\boldsymbol{n}}\times\boldsymbol{F}$). Alternatively, taking the cross product with $\hat{\boldsymbol{n}}$, the N-formulation reads

$$\begin{aligned}\gamma_r\boldsymbol{E}^{inc}(\boldsymbol{r}) &= -\eta\gamma_r\boldsymbol{\mathcal{L}}(\boldsymbol{J}_S)(\boldsymbol{r}) + \gamma_r\boldsymbol{\mathcal{K}}(\boldsymbol{M}_S)(\boldsymbol{r}) - \frac{1}{2}\boldsymbol{M}_S(\boldsymbol{r}),\\ \gamma_r\boldsymbol{H}^{inc}(\boldsymbol{r}) &= -\frac{1}{\eta}\gamma_r\boldsymbol{\mathcal{L}}(\boldsymbol{M}_S)(\boldsymbol{r}) - \gamma_r\boldsymbol{\mathcal{K}}(\boldsymbol{J}_S)(\boldsymbol{r}) + \frac{1}{2}\boldsymbol{J}_S(\boldsymbol{r}).\end{aligned} \tag{4.8}$$

The above formulations can be considered as linear mappings between two Sobolev spaces as [29]

$$\begin{aligned}\text{T-formulation:}\quad & \mathcal{H}_{div}^{-1/2}(S)\times\mathcal{H}_{div}^{-1/2}(S) \;\rightarrow\; \mathcal{H}_{curl}^{-1/2}(S)\times\mathcal{H}_{curl}^{-1/2}(S)\\ \text{N-formulation:}\quad & \mathcal{H}_{div}^{-1/2}(S)\times\mathcal{H}_{div}^{-1/2}(S) \;\rightarrow\; \mathcal{H}_{div}^{-1/2}(S)\times\mathcal{H}_{div}^{-1/2}(S).\end{aligned}$$

However, these are not one-to-one mappings since boundary conditions are not enforced yet.

It is well-known that the above formulations do not give a unique solution at all frequencies when applied for the exterior boundary value problems. The reason is that at certain frequencies, eigenfrequencies of the interior boundary value problem, it is not enough to fix only the tangential components of either electric field or magnetic field at the boundary, and thus, the solution belongs to the null space of the operators [38]. A popular remedy to this problem is to combine the T- and N-formulations as

$$\begin{aligned}\frac{1}{\eta}\gamma_t\boldsymbol{E}^{inc}(\boldsymbol{r})+\gamma_r\boldsymbol{H}^{inc}(\boldsymbol{r}) &= -\gamma_t\boldsymbol{\mathcal{L}}(\boldsymbol{J}_S)(\boldsymbol{r})+\frac{1}{\eta}\gamma_t\boldsymbol{\mathcal{K}}(\boldsymbol{M}_S)(\boldsymbol{r})+\frac{1}{2\eta}\gamma_r\boldsymbol{M}_S(\boldsymbol{r})\\ &\quad -\frac{1}{\eta}\gamma_r\boldsymbol{\mathcal{L}}(\boldsymbol{M}_S)(\boldsymbol{r})-\gamma_r\boldsymbol{\mathcal{K}}(\boldsymbol{J}_S)(\boldsymbol{r})+\frac{1}{2}\boldsymbol{J}_S(\boldsymbol{r}),\\ \eta\gamma_t\boldsymbol{H}^{inc}(\boldsymbol{r})-\gamma_r\boldsymbol{E}^{inc}(\boldsymbol{r}) &= -\gamma_t\boldsymbol{\mathcal{L}}(\boldsymbol{M}_S)(\boldsymbol{r})-\eta\gamma_t\boldsymbol{\mathcal{K}}(\boldsymbol{J}_S)(\boldsymbol{r})-\frac{\eta}{2}\gamma_r\boldsymbol{J}_S(\boldsymbol{r})\\ &\quad +\eta\gamma_r\boldsymbol{\mathcal{L}}(\boldsymbol{J}_S)(\boldsymbol{r})-\gamma_r\boldsymbol{\mathcal{K}}(\boldsymbol{M}_S)(\boldsymbol{r})+\frac{1}{2}\boldsymbol{M}_S(\boldsymbol{r}).\end{aligned} \tag{4.9}$$

The above formulation is known as a combined field integral equation (CFIE) formulation or C-formulation.

4.3 Enforcing the DB boundary condition

The integral equations in (4.7)–(4.9) cannot be solved uniquely as they are. A set of boundary conditions are still needed to reduce the degrees of freedom. Boundary conditions can be enforced by restricting the freedom of the equivalent surface currents. For example, at the PEC boundary, the equivalent magnetic current vanishes because of the boundary condition $\boldsymbol{M}_S=-\boldsymbol{n}\times\boldsymbol{E}=0$, and only the electric current $\boldsymbol{J}_S$ exists.

Enforcing the DB boundary condition is not so straightforward. Using Maxwell's equations and certain vector identities, we can find the following relations between normal components of the fields and surface divergences of the equivalent surface currents:

$$\begin{aligned}\nabla_s \cdot \boldsymbol{J}_S &= \nabla_s \cdot \hat{\boldsymbol{n}} \times \boldsymbol{H} = -\hat{\boldsymbol{n}} \cdot \nabla \times \boldsymbol{H} = i\omega \hat{\boldsymbol{n}} \cdot \boldsymbol{D}, \\ \nabla_s \cdot \boldsymbol{M}_S &= \nabla_s \cdot (-\hat{\boldsymbol{n}} \times \boldsymbol{E}) = \hat{\boldsymbol{n}} \cdot \nabla \times \boldsymbol{E} = i\omega \hat{\boldsymbol{n}} \cdot \boldsymbol{B}.\end{aligned} \tag{4.10}$$

Therefore, on the surface of a DB object, the surface divergences of the equivalent currents vanish (if $\omega \neq 0$), meaning that both the electric $\boldsymbol{J}_S$ and magnetic $\boldsymbol{M}_S$ surface currents must be solenoidal.

In MoM, the unknown equivalent electric $\boldsymbol{J}_S$ and magnetic $\boldsymbol{M}_S$ surface current densities are represented as linear combinations of known tangential vector basis functions $\boldsymbol{f}$ and $\boldsymbol{g}$ as

$$\begin{aligned}\boldsymbol{J}_S &\approx \sum_{k=1}^{N} j_k \boldsymbol{f}_k, \\ \boldsymbol{M}_S &\approx \sum_{l=1}^{M} m_l \boldsymbol{g}_l,\end{aligned} \tag{4.11}$$

where j_k and m_l are scalar coefficients.

Representing both the electric and magnetic equivalent surface current densities with a set of basis functions, which span a solenoidal (null space of divergence operator) vector space, the DB boundary condition is enforced on the surface. In Publications I and II, the DB boundary condition was enforced by using the RWG loop basis functions [39] to expand the equivalent currents, and Galerkin's scheme was used for testing the equations.

It is interesting to note that by enforcing the DB boundary condition for the surface integral equations, the hypersingular term $\nabla \boldsymbol{\mathcal{S}}(\nabla'_S \cdot \boldsymbol{F})$ in the operator $\boldsymbol{\mathcal{L}}$ is identically zero since $\nabla'_S \cdot \boldsymbol{J}_S = 0$ and $\nabla'_S \cdot \boldsymbol{M}_S = 0$. This means that there is no low frequency breakdown nor dense mesh breakdown, which appear in the standard electric field integral equation (EFIE) formulation for PEC objects [38, 40, 41].

In Publication II, field singularities near the DB wedge were studied analytically by solving Laplace's equation in two dimensions, and numerically by MoM in three dimensions. It was concluded that the singularity at the DB wedge is of the same order as it is at the PEC wedge. Therefore, the electromagnetic energy is finite at the DB wedge. For example, in the 90-degree DB wedge, the behavior of field strength is of the form $\rho^{-1/3}$, where ρ is the distance to the wedge when the excitation is antisymmetric.

In a numerical point of view, the field singularities mean that similar mesh refinements are needed near DB wedges as they are near PEC wedges in order to obtain an accurate solution. Fig. 4.2 shows the conver-

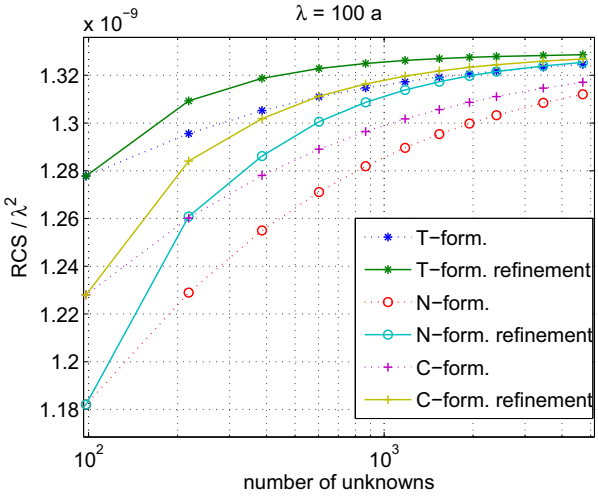

Figure 4.2. Calculated backscattered radar cross section of a cube with edge length a and wavelength $\lambda = 100\,a$ as a function of the number of unknowns [PII]. T-, N-, and C- formulations have been applied. The cube is discretized by using triangular meshes with or without mesh refinement on the edges. Solid lines correspond to the cases with mesh refinements and dotted lines without mesh refinements.

gence of the radar cross section of a DB cube as a function of the number of unknowns. T-, N-, and C-formulations are used either with or without mesh refinements. The discretizations with the mesh refinements give more accurate results than the ones without because of the singularities of the surface currents. It is also notable that the T-formulation is more accurate than the N- or C-formulation. This is because the T-formulation is tested in the dual of the range, but the N-formulation is tested in the range of the operator when Galerkin's testing procedure is applied. Hence, the optimal convergence cannot be achieved with the Galerkin-tested N- or C-formulations.

5. Volume integral equations

A surface integral equation method cannot directly be applied for inhomogeneous and anisotropic materials since the Green function in closed form is not available in a general case. In volume integral equation methods, the Green function is that of background, and hence, it is suitable for scattering problems involving inhomogeneous and anisotropic materials. In this section, three different types of volume integral equation formulations are introduced, and their properties are discussed.

5.1 Volume equivalence principle

Consider an electromagnetic wave scattering by an anisotropic, inhomogeneous, and linear object bounded by a volume V as shown in Fig. 5.1. The permittivity $\bar{\bar{\epsilon}}(\boldsymbol{r})$ and permeability $\bar{\bar{\mu}}(\boldsymbol{r})$ dyadics are functions of position in V. The background is isotropic and homogeneous with the constants ϵ_0 and μ_0.

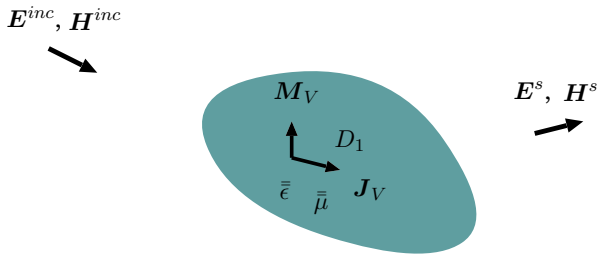

Figure 5.1. Volume equivalence principle: the scatterer is replaced with the volume equivalent currents $\boldsymbol{J}_V$ and $\boldsymbol{M}_V$.

The scattered fields can be expressed by applying the volume equivalence principle in which the scatterer is replaced with the electric and magnetic volume equivalent polarization currents $\boldsymbol{J}_V$ and $\boldsymbol{M}_V$. The total time-harmonic electric $\boldsymbol{E}$ and magnetic $\boldsymbol{H}$ fields can be written as [42]

$$\boldsymbol{E}(\boldsymbol{r}) = \boldsymbol{E}^{\text{inc}}(\boldsymbol{r}) + \frac{-1}{i\omega\epsilon_0}\left(\nabla\nabla + k_0^2\bar{\bar{I}}\right)\cdot\boldsymbol{\mathcal{S}}(\boldsymbol{J}_V)(\boldsymbol{r}) - \nabla\times\boldsymbol{\mathcal{S}}(\boldsymbol{M}_V)(\boldsymbol{r}), \quad (5.1)$$

$$\boldsymbol{H}(\boldsymbol{r}) = \boldsymbol{H}^{\text{inc}}(\boldsymbol{r}) + \frac{-1}{i\omega\mu_0}\left(\nabla\nabla + k_0^2\bar{\bar{I}}\right)\cdot\boldsymbol{\mathcal{S}}(\boldsymbol{M}_V)(\boldsymbol{r}) + \nabla\times\boldsymbol{\mathcal{S}}(\boldsymbol{J}_V)(\boldsymbol{r}). \quad (5.2)$$

Here, $\boldsymbol{E}^{inc}$ and $\boldsymbol{H}^{inc}$ are the incident electric and magnetic fields with sources outside the domain V, and $k_0 = \omega\sqrt{\epsilon_0\mu_0}$ is the wave number in the background. The equivalent polarization currents are defined as

$$\boldsymbol{J}_V(\boldsymbol{r}) = -i\omega\epsilon_0\bar{\bar{\tau}}_\epsilon(\boldsymbol{r})\cdot\boldsymbol{E}(\boldsymbol{r}) = -i\omega\bar{\bar{\chi}}_\epsilon(\boldsymbol{r})\cdot\boldsymbol{D}(\boldsymbol{r}), \quad (5.3)$$

$$\boldsymbol{M}_V(\boldsymbol{r}) = -i\omega\mu_0\bar{\bar{\tau}}_\mu(\boldsymbol{r})\cdot\boldsymbol{H}(\boldsymbol{r}) = -i\omega\bar{\bar{\chi}}_\mu(\boldsymbol{r})\cdot\boldsymbol{B}(\boldsymbol{r}), \quad (5.4)$$

in which

$$\bar{\bar{\tau}}_\epsilon(\boldsymbol{r}) = \bar{\bar{\epsilon}}_r(\boldsymbol{r}) - \bar{\bar{I}}, \quad (5.5)$$

$$\bar{\bar{\tau}}_\mu(\boldsymbol{r}) = \bar{\bar{\mu}}_r(\boldsymbol{r}) - \bar{\bar{I}}, \quad (5.6)$$

$$\bar{\bar{\chi}}_\epsilon(\boldsymbol{r}) = \bar{\bar{I}} - \bar{\bar{\epsilon}}_r^{-1}(\boldsymbol{r}), \quad (5.7)$$

$$\bar{\bar{\chi}}_\mu(\boldsymbol{r}) = \bar{\bar{I}} - \bar{\bar{\mu}}_r^{-1}(\boldsymbol{r}), \quad (5.8)$$

where $\bar{\bar{\epsilon}}_r$ and $\bar{\bar{\mu}}_r$ are the relative permittivity and permeability dyadics, respectively, and $\bar{\bar{I}}$ is the identity dyadic. The volume integral operator in (5.1) and (5.2) is

$$\boldsymbol{\mathcal{S}}(\boldsymbol{F})(\boldsymbol{r}) = \int_V G_0(\boldsymbol{r},\boldsymbol{r}')\,\boldsymbol{F}(\boldsymbol{r}')\,dV', \quad (5.9)$$

where G_0 is the Green function of the background

$$G_0(\boldsymbol{r},\boldsymbol{r}') = \frac{e^{ik_0|\boldsymbol{r}-\boldsymbol{r}'|}}{4\pi|\boldsymbol{r}-\boldsymbol{r}'|}. \quad (5.10)$$

5.2 Volume integral equation formulations

Three different types of formulations can be derived from (5.1) and (5.2). The most widely used formulation is the so-called DB-formulation in which the flux densities $\boldsymbol{D}$ and $\boldsymbol{B}$ are the unknowns [43, 44]. By representing the equivalent currents in terms of the flux densities and substituting them into (5.1) and (5.2), the DB-formulation is obtained:

$$\begin{aligned}\boldsymbol{D}^{\text{inc}} &= \bar{\bar{\epsilon}}_r^{-1}\cdot\boldsymbol{D} - (\nabla\nabla + k_0^2\bar{\bar{I}})\cdot\boldsymbol{\mathcal{S}}(\bar{\bar{\chi}}_\epsilon\cdot\boldsymbol{D}) - i\omega\epsilon_0\nabla\times\boldsymbol{\mathcal{S}}(\bar{\bar{\chi}}_\mu\cdot\boldsymbol{B}),\\ \boldsymbol{B}^{\text{inc}} &= \bar{\bar{\mu}}_r^{-1}\cdot\boldsymbol{B} - (\nabla\nabla + k_0^2\bar{\bar{I}})\cdot\boldsymbol{\mathcal{S}}(\bar{\bar{\chi}}_\mu\cdot\boldsymbol{B}) + i\omega\mu_0\nabla\times\boldsymbol{\mathcal{S}}(\bar{\bar{\chi}}_\epsilon\cdot\boldsymbol{D}).\end{aligned} \quad (5.11)$$

The volume integral equation formulation for the electric and magnetic fields can be obtained by using the fact that

$$(\nabla\nabla + k_0^2\bar{\bar{I}}) \cdot \boldsymbol{\mathcal{S}}(\boldsymbol{F}) = \nabla \times (\nabla \times \boldsymbol{\mathcal{S}}(\boldsymbol{F})) - \boldsymbol{F}, \tag{5.12}$$

and analogously, representing the unknowns in terms of the fields $\boldsymbol{E}$ and $\boldsymbol{H}$, the EH-formulation [45, 46] can be written as follows:

$$\begin{aligned} \boldsymbol{E}^{\text{inc}} &= \bar{\bar{\epsilon}}_r \cdot \boldsymbol{E} - \nabla \times \nabla \times \boldsymbol{\mathcal{S}}(\bar{\bar{\tau}}_\epsilon \cdot \boldsymbol{E}) - i\omega\mu_0 \nabla \times \boldsymbol{\mathcal{S}}(\bar{\bar{\tau}}_\mu \cdot \boldsymbol{H}), \\ \boldsymbol{H}^{\text{inc}} &= \bar{\bar{\mu}}_r \cdot \boldsymbol{H} - \nabla \times \nabla \times \boldsymbol{\mathcal{S}}(\bar{\bar{\tau}}_\mu \cdot \boldsymbol{H}) + i\omega\epsilon_0 \nabla \times \boldsymbol{\mathcal{S}}(\bar{\bar{\tau}}_\epsilon \cdot \boldsymbol{E}). \end{aligned} \tag{5.13}$$

In a third type of formulation, the equations are written for the unknown equivalent polarization currents $\boldsymbol{J}_V$ and $\boldsymbol{M}_V$. We call this formulation as a JM-formulation, and it reads as

$$\begin{aligned} \boldsymbol{J}_V^{\text{inc}} &= \boldsymbol{J}_V - \bar{\bar{\tau}}_\epsilon \cdot (\nabla\nabla + k_0^2\bar{\bar{I}}) \cdot \boldsymbol{\mathcal{S}}(\boldsymbol{J}_V) - i\omega\epsilon_0 \bar{\bar{\tau}}_\epsilon \cdot \nabla \times \boldsymbol{\mathcal{S}}(\boldsymbol{M}_V), \\ \boldsymbol{M}_V^{\text{inc}} &= \boldsymbol{M}_V - \bar{\bar{\tau}}_\mu \cdot (\nabla\nabla + k_0^2\bar{\bar{I}}) \cdot \boldsymbol{\mathcal{S}}(\boldsymbol{M}_V) + i\omega\mu_0 \bar{\bar{\tau}}_\mu \cdot \nabla \times \boldsymbol{\mathcal{S}}(\boldsymbol{J}_V), \end{aligned} \tag{5.14}$$

or

$$\begin{aligned} \boldsymbol{J}_V^{\text{inc}} &= \bar{\bar{\epsilon}}_r \cdot \boldsymbol{J}_V - \bar{\bar{\tau}}_\epsilon \cdot \nabla \times \nabla \times \boldsymbol{\mathcal{S}}(\boldsymbol{J}_V) - i\omega\epsilon_0 \bar{\bar{\tau}}_\epsilon \cdot \nabla \times \boldsymbol{\mathcal{S}}(\boldsymbol{M}_V), \\ \boldsymbol{M}_V^{\text{inc}} &= \bar{\bar{\mu}}_r \cdot \boldsymbol{M}_V - \bar{\bar{\tau}}_\mu \cdot \nabla \times \nabla \times \boldsymbol{\mathcal{S}}(\boldsymbol{M}_V) + i\omega\mu_0 \bar{\bar{\tau}}_\mu \cdot \nabla \times \boldsymbol{\mathcal{S}}(\boldsymbol{J}_V). \end{aligned} \tag{5.15}$$

The above JM-formulations are equivalent in L^2.

5.3 Properties of formulations

The main difference in the above-mentioned formulations is the quantity of unknowns—that is, the flux densities in the DB-formulation, the fields in the EH-formulation, and the equivalent volume currents in the JM-formulation. Applying these formulations to media with extreme parameters can be detrimental to the condition of the system. As discussed in [30] and [47], the well-posedness of the formulations depends on the permittivity and permeability functions. They should be coercive and bounded:

$$a \langle \boldsymbol{f}, \boldsymbol{f} \rangle \leq \langle \boldsymbol{f}, \epsilon \boldsymbol{f} \rangle \leq b \langle \boldsymbol{f}, \boldsymbol{f} \rangle, \tag{5.16}$$

for some $0 < a, b < \infty$ and any $\boldsymbol{f} \in L^2$. At the limits $\epsilon = 0$ or $\epsilon = \infty$, these conditions are not valid, and therefore, the JM-, DB-, and EH-formulations are not equivalent in the sense of the existence and uniqueness of the solution. The above analysis is also valid for the permeability μ.

Publication IV studies the behaviors of these formulations in the case of extremely anisotropic materials. It turns out that only the JM-formulation is stable and gives the most accurate solution at a wide range of material parameters. Because of the constitutive relations $\boldsymbol{D} = \epsilon \boldsymbol{E}$ and $\boldsymbol{B} = \mu \boldsymbol{H}$ and the finite energy assumption, we can point out the following about the flux densities and the fields at extreme cases:

$$\begin{aligned} \lim_{\epsilon \to 0} \boldsymbol{D} = 0, \quad \lim_{\mu \to 0} \boldsymbol{B} = 0, \\ \lim_{\epsilon \to \infty} \boldsymbol{E} = 0, \quad \lim_{\mu \to \infty} \boldsymbol{H} = 0. \end{aligned} \tag{5.17}$$

In the DB-formulation, the unknown flux densities vanish when $\epsilon \to 0$ and $\mu \to 0$, and the system becomes unstable. The same thing happens to the EH-formulation when $\epsilon \to \infty$ and $\mu \to \infty$. The equivalent volume currents, on the other hand, are linear combinations of the fluxes and fields, and hence, the unknowns in the JM-formulation do not vanish in the case of extreme medium.

From the numerical point of view, the main difference in these formulations is the choice of basis and testing functions. Basis functions are used for representing the unknowns; hence, they should satisfy the continuity conditions of the unknowns. In particular, it is crucial not to enforce any extra continuities. In other words, basis functions should span a proper vector space. As pointed out in [30], [33], and [47] to guarantee the convergence in the norm of the solution, it is essential that testing functions span the L^2 dual space of the range of the integral operator. The mapping properties of the equations read as follows

$$\begin{aligned} &\text{DB-formulation:} && \mathcal{H}_{div}(\Omega) \times \mathcal{H}_{div}(\Omega) && \to && \mathcal{H}_{curl}(\Omega) \times \mathcal{H}_{curl}(\Omega), \\ &\text{EH-formulation:} && \mathcal{H}_{curl}(\Omega) \times \mathcal{H}_{curl}(\Omega) && \to && \mathcal{H}_{div}(\Omega) \times \mathcal{H}_{div}(\Omega), \\ &\text{JM-formulation:} && L^2(\Omega) \times L^2(\Omega) && \to && L^2(\Omega) \times L^2(\Omega). \end{aligned}$$

Since $\mathcal{H}_{div}$ and $\mathcal{H}_{curl}$ are L^2 duals to each other and the L^2 is dual to itself, the equations are tested in the dual spaces of the ranges when Galerkin's testing is applied. However, when the local basis and testing functions are applied, it is not clear that the standard testing functions span the actual dual space of the range of the discrete operator. This could lead to a solution space larger than the intended one [30]. To overcome this problem, the local testing functions should be constructed carefully or work fully in L^2 by using the JM-formulation as suggested in [30].

Publication IV demonstrates numerically that the JM-formulation is

stable in terms of the system condition when discretized with piecewise constant basis and testing functions, whereas the standard discretizations of the DB- and EH-formulations suffer from the breakdown in the case of a highly anisotropic medium. Fig. 5.2 shows the number of GM-

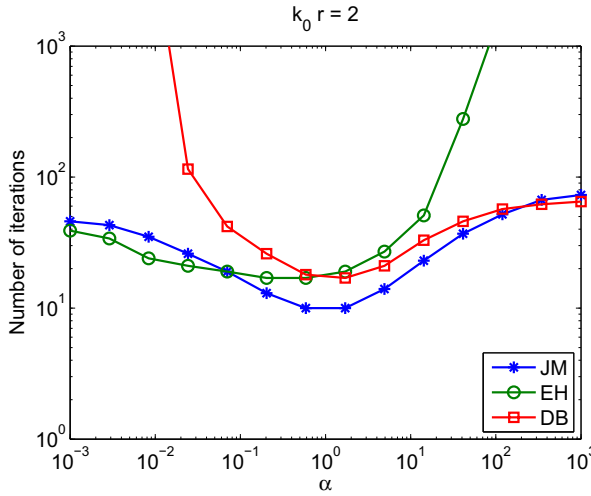

Figure 5.2. Number of iterations required to solve the system as a function of radial permittivity [PIV].

RES iterations required to solve the linear system as a function of radial permittivity. The stopping criterion of GMRES is 10^{-4}. With increasing radial permittivity, the EH-formulation becomes unstable, and the DB-formulation breaks down when the axial permittivity tends to zero. The JM-formulation is the most stable one in this case. Similar observations have been made for objects of different shapes and sizes in Publication IV.

6. Material approximations for DB and D′B′ boundaries

In this section, we study numerically how well certain extreme materials approximate the ideal DB and D′B′ boundaries. Material approximations are not unique, and here, we only consider simple materializations with the isotropic or anisotropic permittivity and permeability (bianisotropy is not allowed). By the term "materialization", we mean an interface of two media with given material parameters that approximate the ideal mathematical boundary. Another step of realization is to find practical metamaterial elements that produce effective material parameters which would mimic the mathematical boundary condition.

6.1 DB boundary

The DB boundary can be materialized with an interface between the free space and a uniaxial medium in which the normal components of the permittivity and permeability dyadics vanish:

$$\hat{\boldsymbol{n}} \cdot \bar{\bar{\epsilon}} = 0, \;\; \hat{\boldsymbol{n}} \cdot \bar{\bar{\mu}} = 0, \tag{6.1}$$

while the transverse components $(\bar{\bar{I}} - \hat{\boldsymbol{n}}\hat{\boldsymbol{n}}) \cdot \bar{\bar{\epsilon}}$ and $(\bar{\bar{I}} - \hat{\boldsymbol{n}}\hat{\boldsymbol{n}}) \cdot \bar{\bar{\mu}}$ do not affect the fields outside the object at all [25]. If the conditions of (6.1) are not exactly zero, the scattered fields are affected by the transverse components. Materials with zero permittivity and permeability have been of great interest among the metamaterial community [48, 49]. A realization of a metamaterial unit shell that produces the material parameters with zero axial permittivity and permeability can be found in [50, 51].

The zero axial medium, however, is not the only possible material approximation. It has been shown that a material interface of the so-called skewon-axion medium or its generalization, the P-medium, also mimics the DB boundary [52]. The materialization with the skewon-axion

medium would require bianisotropic materials, and hence, it is out of the scope of this thesis.

First, we investigate how close to zero the permittivity and permeability have to be to approximate the ideal DB boundary. Fig. 6.1 shows the relative difference in the total scattering cross section of a sphere. Two materializations are considered. The isotropic approximation in which

$$\bar{\bar{\epsilon}} = \alpha\epsilon_0\bar{\bar{I}}, \quad \bar{\bar{\mu}} = \alpha\mu_0\bar{\bar{I}}, \tag{6.2}$$

and the radially uniaxial approximation, with

$$\begin{aligned} \bar{\bar{\epsilon}} &= \alpha\epsilon_0\boldsymbol{u}_r\boldsymbol{u}_r + \epsilon_0\boldsymbol{u}_\theta\boldsymbol{u}_\theta + \epsilon_0\boldsymbol{u}_\phi\boldsymbol{u}_\phi, \\ \bar{\bar{\mu}} &= \alpha\mu_0\boldsymbol{u}_r\boldsymbol{u}_r + \mu_0\boldsymbol{u}_\theta\boldsymbol{u}_\theta + \mu_0\boldsymbol{u}_\phi\boldsymbol{u}_\phi. \end{aligned} \tag{6.3}$$

The total scattering cross sections as functions of material parameters are obtained by the exact Mie solution for either the isotropic or uniaxially anisotropic spheres [53, 54]. The reference result for the ideal DB sphere can also be calculated by Mie expansion [3].

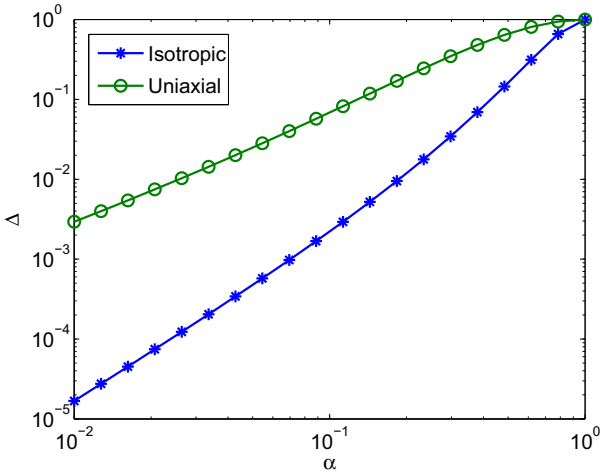

Figure 6.1. A relative difference in the total scattering cross section between the ideal DB sphere of size $ka = 2$ and its material approximation either with the isotropic or radially uniaxial material [PIV].

The results in Fig. 6.1 show that the isotropic material with a small permittivity and permeability yields a better approximation of the ideal DB boundary than the uniaxial material. Nevertheless, with decreasing α the far field scattering of both materials approaches to that of the sphere with the ideal DB boundary. The field distributions outside are the same when α is exactly zero.

As discussed in Publication II, nonsmooth DB scatterers with sharp

wedges and corners can create field singularities. Therefore, it is important to look at the fields near a nonsmooth scatterer.

We construct a cube that mimics the ideal DB cube from six blocks in which the permittivities and permeabilities are defined, as shown in Fig. 6.2.

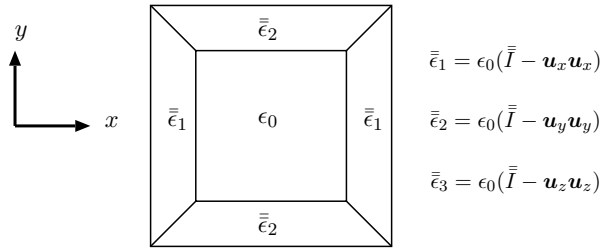

Figure 6.2. A cross section of a cube that approximates the ideal DB cube [PIV]. The cube is built from six blocks in order to define the material parameters in which the components normal to the interface vanish. The permeability $\bar{\bar{\mu}}$ is defined analogously to the permittivity $\bar{\bar{\epsilon}}$, except ϵ_0 is replaced with μ_0.

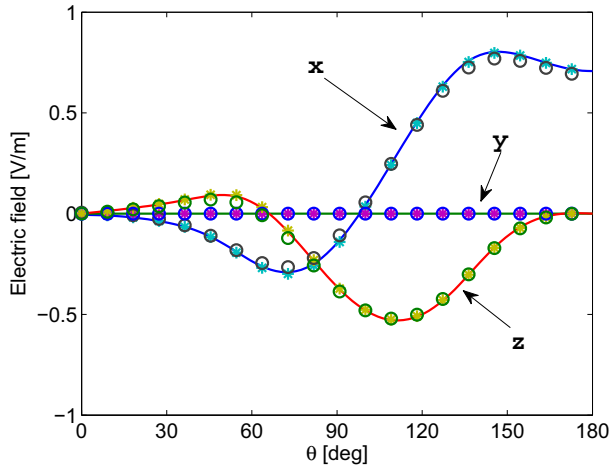

Figure 6.3. The x-, y-, and z-components of the real part of the electric field near the cube on the electric field plane (xz-plane) [PIV]. The solid curves denote the ideal DB cube, and stars and circles designate the isotropic and anisotropic approximations of the DB cube, respectively. The backscattering direction is at $\theta = 0$ deg.

The edge length of the cube is $l = 1\,\text{m}$, and the thicknesses of the blocks are $0.1\,\text{m}$. The cube is illuminated by the x-polarized plane wave with the frequency $f = 2\,\text{GHz}$ propagating along the z-axis. Fig. 6.3 illustrates the x-, y-, and z-components of the real part of the electric field calculated in the electric field plane (xz-plane) at a distance $r = 1\,\text{m}$ from the center of the cube. The computations are done for the ideal DB cube by using the surface integral equation C-formulation for the ideal DB boundary (solid

lines). For the isotropic (stars) and anisotropic (circles) approximations, the volume integral equation JM-formulation is used.

The near field patterns of two approximations and the ideal DB cube show good agreements. We observe a small deviation between the ideal DB cube and the uniaxial approximation. For the numerical point of view, the uniaxial approximation is a more challenging problem since the fields decay exponentially inside the cube, and therefore, the difference is mainly due to the inaccuracy of the numerical solution. The accuracy of the numerical solution can be improved by increasing the discretization density near the surface where the fields decay exponentially. In addition, the wedges and corners of the uniaxial approximation may create some minor differences to the fields near wedges, but overall, the scattering properties are almost equivalent.

6.2 D′B′ boundary

Let us next consider the D′B′ sphere of radius $r = 1\,\mathrm{m}$, and an incident plane wave with the wavelength $\lambda_0 = 3.2\,\mathrm{m}$. The DB boundary can be transformed to the D′B′ boundary by a quarter-wave transformer (a quarter-wavelength layer of the wave-guiding medium) as shown in Publication V and [55]. The wave-guiding effect can be obtained with a uniaxial material by letting the axial components of the permittivity and permeability tend to infinity. This property forces the fields to be perpendicular to the axis of propagation, meaning that the wave is of a transverse electromagnetic (TEM) type for all excitations. Thus, the thickness of the layer is independent of excitation, and the quarter-wave transformer can be obtained.

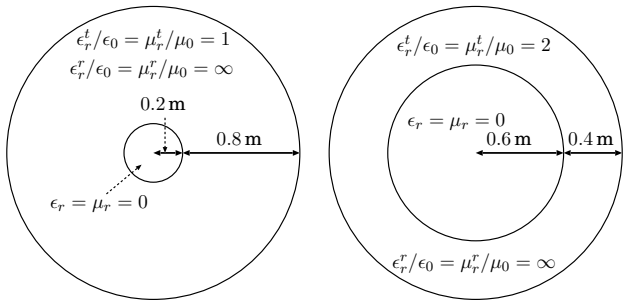

Figure 6.4. Two possible approximations for the spherical D′B′ boundary [PV]. The spherical D′B′ boundary can be realized with the transformer layer upon the DB sphere. The thickness of the layer can be controlled by the transverse components of the permittivity ϵ_r^t and permeability μ_r^t.

Fig. 6.4 presents two possible materializations for the D′B′ sphere with different transverse parameters ϵ_r^t, μ_r^t. Since the wavelength inside the wave-guiding medium depends only on the transverse components of the medium parameters, the thickness of the quarter-wave transformer layer is $0.8\,\mathrm{m}$ when $\epsilon_r^t/\epsilon_0 = \mu_r^t/\mu_0 = 1$, and when $\epsilon_r^t/\epsilon_0 = \mu_r^t/\mu_0 = 2$, the layer thickness is reduced to $0.4\,\mathrm{m}$. To obtain the DB condition on the surface of the inner sphere, the permittivity and permeability of the inner sphere are set to zero ($\epsilon_r = \mu_r = 0$).

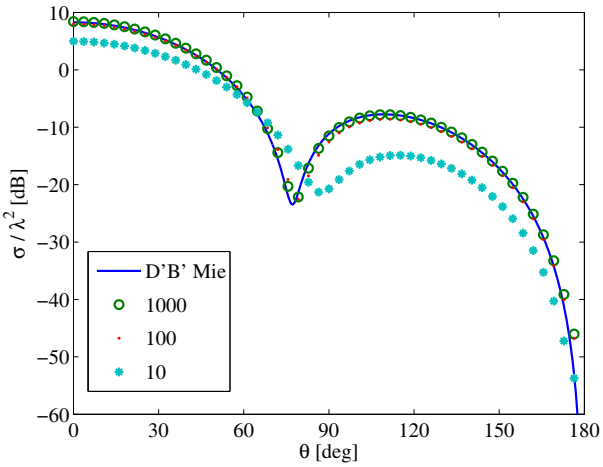

Figure 6.5. Scattering cross sections of the materializations of the D′B′ spheres [PV]. The scatterer is presented in Fig. 6.4 (left). Different values of the radial permittivity and permeability $\epsilon_r^r/\epsilon_0 = \mu_r^r/\mu_0$ are used to approximate the quarter-wave transformer. The backscattering direction is at $\theta = 180$ deg.

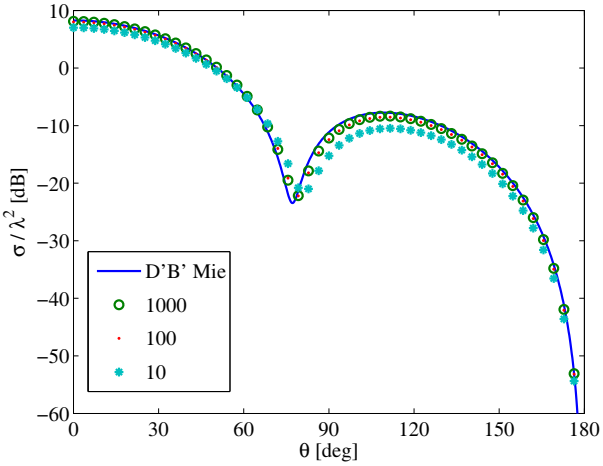

Figure 6.6. Scattering cross sections of the material approximations of the D′B′ spheres [PV]. The scatterer is presented in Fig. 6.4 (right).

Figs. 6.5 and 6.6 show scattering cross sections (SCS) of the coated

spheres corresponding to those in Fig. 6.4 calculated by using the volume integral equation method with the JM-formulation. The reference result for the ideal D′B′ sphere is computed by the exact Mie solution [3]. Both realizations approximate the ideal D′B′ sphere when the radial components of the material parameters grow large in amplitude. However, this material approximation cannot directly be applied for arbitrarily shaped objects. In particular, materializations of sharp wedges or corners without rounding them cannot be obtained with the material approximation based on the quarter-wave transformer. It is also notable that since this approximation is based on the electrical thickness of the layer, the bandwidth cannot be very large. In addition, one should remember that material parameters are functions of frequency; hence, the bandwidth is also restricted by causality.

7. Novelty of research and summary of the publications

In this thesis, we developed a numerical method based on surface integral equations to analyze scattering problems involving arbitrarily shaped 3-D objects with the DB boundary condition. Such a method has not been available before. The developed method was then used to obtain better understanding of scattering properties of objects with the DB boundary condition.

We also presented a systematic analysis of different types of volume integral equation formulations for general dielectric and magnetic materials, as well as a new discretization of a volume integral equation formulation. The scheme was shown to be more stable in terms of conditioning of the system compared with standard schemes, especially when the material parameters are strongly anisotropic.

The developed method was used for examining approximations of the ideal DB and D′B′ boundary conditions in terms of strongly anisotropic materials. Finally, the method was accelerated by a multilevel fast multipole algorithm (MLFMA), and applied to the three-dimensional cloaking structure.

Publication I: "Computation of scattering by DB objects with surface integral equation method"

The first paper studies the electromagnetic wave scattering of objects whose surface is characterized by the DB boundary condition. At the DB boundary, normal components of the electric and magnetic flux densities vanish.

A numerical method, based on surface integral equations, is developed for solving scattering problems involving arbitrarily shaped three-dimensional objects with the DB boundary condition. The surface integral equa-

tions are discretized by the method of moments. It is shown that requiring the unknown electric and magnetic surface currents to be solenoidal is equivalent to enforcing the DB boundary condition. The unknown surface current densities have been expanded with solenoidal basis functions, known as loop functions. This solenoidal basis can be constructed from the standard RWG basis by combining these basis functions properly.

The developed method is validated by investigating the scattering properties of spheres, in which case the analytical solution is available. It is shown that the developed method does not suffer from the low frequency breakdown, and thus, analyzing almost static phenomena is possible. Moreover, the paper describes how to determine the polarizabilities of DB objects of arbitrary shape by using a dynamical solver. Finally, the paper discusses the uniqueness of the solution in the case of multiply connected objects.

Publication II: "Surface integral equation method for scattering by DB objects with sharp wedges"

This paper focuses on the field singularities at the DB wedge. A two-dimensional quasi-static field solution is derived near the sharp DB wedge by solving Laplace's equation with the DB boundary condition in the polar coordinate system. The analysis shows that the strength of the singularity at the DB wedge is of the same order as that of at the PEC wedge. However, different components of the field can be singular. At the DB wedge, only the tangential components of fields can be singular, whereas at the PEC wedge, both the normal and tangential components of fields can be singular depending on excitation. Furthermore, the accuracy of the surface integral equation solution, proposed in Publication I, in the presence of the DB wedges is investigated. It appears that mesh refinements are needed near the DB wedges in order to obtain an accurate solution, which is a well-known result in the case of the PEC boundary condition.

Publication III: "Analysis of volume integral equation formulations for scattering by high-contrast penetrable objects"

This paper analyzes the properties of different volume integral equation formulations for electromagnetic wave scattering. Special attention is paid for the behavior of these formulations when the material parame-

ters grow large in amplitude. It is concluded that the accuracy of the volume magnetic field integral equation (VMFIE) is very poor compared with other discretizations of the volume integral equations. Previously, it was reported that VMFIE is as accurate as the other formulations; however, in this paper, it is shown that this is only true for low-contrast objects. With increasing permittivity contrast, the accuracy of VMFIE becomes poor. The reason for this is found to be that VMFIE is tested in the range space of the integral operator when Galerkin's method is applied. The formulations, which are tested in the dual spaces of the ranges, give more accurate results. Hence, by constructing a proper set of testing functions, the accuracy of VMFIE could be improved.

Publication IV: "Discretization of volume integral equation formulations for extremely anisotropic materials"

The purpose of this paper is twofold: first, to present a stable discretization of the volume integral equation formulation for extremely anisotropic media, and second, to analyze material realization of the DB boundary based on a highly anisotropic material interface.

A discretization of the JM-formulation, which is based on equivalent polarization currents, is presented. The currents are expanded with piecewise constant basis functions which allow the accurate modeling of highly anisotropic media. It is demonstrated that the JM-formulation is stable in the presence of extremely anisotropic media, whereas the more conventional volume integral equation formulations, based on the fields or fluxes, suffer from breakdown.

The second part analyzes electromagnetic properties of material approximations of the DB boundary. Two approximations are considered. One is based on a uniaxially anisotropic material with vanishing axial components of the permittivity and permeability dyadics, and the other is a simple isotropic approximation with zero permittivity and permeability. Both material realizations are found to approximate the ideal DB boundary.

Publication V: "Realization of spherical D′B′ boundary by a layer of wave-guiding medium"

This paper discusses the material approximation of the spherical D′B′ boundary by a layer of wave-guiding medium. The wave-guiding medium is obtained by letting the radial components of the permittivity and permeability dyadics grow to infinity. It is shown that a quarter-wavelength layer of such a medium, known as a quarter-wave transformer, lying on the surface of a DB sphere mimics the ideal D′B′ boundary. The theory is tested numerically by solving the scattering from a DB sphere coated with a layer of wave-guiding medium. Then the results are compared with the scattering of the corresponding ideal D′B′ sphere.

The DB boundary is approximated by a material with zero permittivity and permeability. This means that materials with extreme parameters are required, and thus, a stable numerical algorithm is needed to solve the problem. The volume integral equation method based on equivalent volume currents, developed in Publication IV, is used in the calculations.

Publication VI: "Broadband multilevel fast multipole algorithm for electric-magnetic current volume integral equation"

A multilevel fast multipole algorithm (MLFMA) is applied to accelerate a volume integral equation solution. The volume integral equations are formulated in terms of equivalent volume currents, which are expanded with piecewise constant approximations. In Publication IV, it was shown that this formulation is more stable than conventional ones when material parameters are extremely anisotropic, and thus, suitable for acceleration with MLFMA.

The developed solver utilizes a broadband version of the MLFMA—that is, at the subwavelength levels, spectral translators are used, and at the superwavelength levels, standard high-frequency MLFMA is applied. Moreover, improved global interpolations based on trigonometric polynomials are used to reduce the number of sample points compared with the previous implementations. This also leads to an excellent accuracy control when a high number of successive interpolations is required.

Finally, it is shown that the developed method allows efficient and accurate modeling of bodies with strongly inhomogeneous and anisotropic responses (for example, cloaking devices).

Bibliography

[1] J. C. Maxwell. On physical lines of force, parts 1-4. *Philosophical Magazine*, 21, 23, 1861-1862.

[2] J. C. Maxwell. A dynamical theory of the electromagnetic field. *Philosophical Transactions of the Royal Society of London*, 4:459–512, 1865.

[3] I.V. Lindell, A. Sihvola, P. Ylä-Oijala, and H. Wallén. Zero backscattering from self-dual objects of finite size. *IEEE Transactions on Antennas and Propagation*, 57(9):2725–2731, Sept. 2009.

[4] I.V. Lindell and A. Sihvola. Electromagnetic boundary conditions defined in terms of normal field components. *IEEE Transactions on Antennas and Propagation*, 58(4):1128–1135, Apr. 2010.

[5] P.-S. Kildal. Definition of artificially soft and hard surfaces for electromagnetic waves. *Electronics Letters*, 24(3):168–170, 1988.

[6] P-S. Kildal. Artificially soft and hard surfaces in electromagnetics. *IEEE Transactions on Antennas and Propagation*, 38(10):1537–1544, 1990.

[7] I. V. Lindell and A. H. Sihvola. Electromagnetic boundary and its realization with anisotropic metamaterial. *Physical Review E*, 79:026604, Feb. 2009.

[8] M. Lapine and S. Tretyakov. Contemporary notes on metamaterials. *IET Microwaves, Antennas and Propagation*, 1(1):3–11, Feb. 2007.

[9] A. Sihvola. Metamaterials: A personal view. *Radioengineering*, 18(2):90–94, Jun. 2009.

[10] A. Alù, N. Engheta, A. Erentok, and R. W. Ziolkowski. Single-negative, double-negative, and low-index metamaterials and their electromagnetic applications. *IEEE Antennas and Propagation Magazine*, 49(1):23–36, Feb. 2007.

[11] P-S. Kildal, A.A. Kishk, and S. Maci. Special issue on artificial magnetic conductors, soft/hard surfaces, and other complex surfaces. *IEEE Transactions on Antennas and Propagation*, 53(1):2–7, 2005.

[12] P-S. Kildal. Fundamental properties of canonical soft and hard surfaces, perfect magnetic conductors and the newly introduced DB surface and their relation to different practical applications including cloaking. *International Conference on Electromagnetics in Advanced Applications, 2009. ICEAA 09*, pages 607–610, 2009.

[13] J. B. Pendry, D. Schurig, and D. R. Smith. Controlling electromagnetic fields. *Science*, 312(5781):1780–1782, Jun. 2006.

[14] B. Zhang, H. Chen, B. I. Wu, and J.A. Kong. Extraordinary surface voltage effect in the invisibility cloak with an active device inside. *Physical Review Letters*, 100, 063904-1-4, Feb. 2008.

[15] E. Martini, S. Maci, and A. D. Yaghjian. DB boundary conditions at the inner surface of an arbitrarily shaped cloak. *Proceedings of the 5th European Conference on Antennas and Propagation (EuCAP)*, pages 3453–3455, 11-15 Apr. 2011.

[16] E. Martini, S. Maci, and A. Yaghjian. *Cloaking in terms of nonradiating cancelling currents -Selected topics in photonic crystals and metamaterials*. Edited by V Galdi, World Scientific, 2011.

[17] G. Mie. Beiträge zur optik trüber medien, speziell kolloidaler metallösungen. *Annalen der Physik*, 25:377–445, 1908.

[18] J. D. Jackson. *Classical Electrodynamics*. New York, John Wiley & Sons, 3 edition, 1999.

[19] N. W. Ashcroft and Mermin N. D. *Solid state physics*. New York, Holt, 1 edition, 1976.

[20] J. S. Toll. Causality and the dispersion relation: Logical foundations. *Physical Review*, 104:1760–1770, Dec. 1956.

[21] T. B. A. Senior and J.L. Volakis. *Approximative boundary conditions in electromagnetics*. The Institution of Electrical Engineering, London, 1 edition, 1995.

[22] G. Pelosi and P. Y. Ufimtsev. The impedance boundary condition. *IEEE Antennas and Propagation Magazine*, 38:31–35, 1996.

[23] I. V. Lindell. *Methods for Electromagnetic Field Analysis*. New York, IEEE Press, 2 edition, 1995.

[24] I.V. Lindell and A. Sihvola. Perfect electromagnetic conductor. *Journal of Electromagnetic Waves and Applications*, 19(7):861–869, 2005.

[25] V. Rumsey. Some new forms of Huygens' principle. *IRE Transactions on Antennas and Propagation*, 7(5):103–116, Dec. 1959.

[26] K. S. Yee. Uniqueness theorems for an exterior electromagnetic field. *SIAM Journal on Applied Mathematics*, 18(1):77–83, Jan. 1970.

[27] R. Kress. On an exterior boundary-value problem for the time-harmonic Maxwell equations with boundary conditions for the normal components of the electric and magnetic field. *Mathematical Methods in the Applied Sciences*, 8:77–92, 1986.

[28] R. F. Harrington. *Field Computation by Moment Methods*, volume 1. IEEE press, New York, 1993.

[29] G.C. Hsiao and R. E. Kleinman. Mathematical foundations for error estimation in numerical solutions of integral equations in electromagnetics. *IEEE Transactions on Antennas and Propagation*, 45(3):316–328, Mar. 1997.

[30] M.C. van Beurden and S. J.L. van Eijndhoven. Gaps in present discretization schemes for domain integral equations. *International Conference on Electromagnetics in Advanced Applications, ICEAA 2007, Torino*, 2007.

[31] A. Buffa and P. Ciarlet Jr. On traces for functional spaces related to Maxwell's equations part I: An integration by parts formula in Lipschitz polyhedra. *Mathematical Methods in the Applied Sciences*, 24:9–30, 2001.

[32] S. Rao, D. Wilton, and A. Glisson. Electromagnetic scattering by surfaces of arbitrary shape. *IEEE Transactions on Antennas and Propagation*, 30(3):409–418, May 1982.

[33] Z. Chen and Y. Xu. The Petrov-Galerkin and iterated Petrov-Galerkin methods for second-kind integral equations. *Journal on Numerical Analysis*, 35(1):406–434, Feb. 1998.

[34] Ö. Ergül and L. Gürel. Improving the accuracy of the magnetic field integral equation with the linear-linear basis functions. *Radio Science*, 41(4), 2006.

[35] K. Cools, F.P. Andriulli, D. De Zutter, and E. Michielssen. Accurate and conforming mixed discretization of the MFIE. *IEEE Antennas and Wireless Propagation Letters*, 10:528–531, 2011.

[36] P. Ylä-Oijala, S.P. Kiminki, K Cools, F.P. Andriulli, and S. Järvenpää. Mixed discretizations schemes for electromagnetic surface integral equations. *International Journal of Numerical Modeling*, 25:525–540, Jan. 2012.

[37] J. A. Stratton. *Electromagnetic Theory*, volume 1. McGraw-Hill Company, New York, London, 1941.

[38] D. Colton and R. Kress. *Integral equation methods in scattering theory*. John Wiley, New York, 1983.

[39] G. Vecchi. Loop-star decomposition of basis functions in the discretization of the EFIE. *IEEE Transactions on Antennas and Propagation*, 47(2):339–346, Feb. 1999.

[40] J.-S. Zhao and W.C. Chew. Integral equation solution of Maxwell's equations from zero frequency to microwave frequencies. *IEEE Transactions on Antennas and Propagation*, 48(10):1635–1645, Oct. 2000.

[41] R.J. Adams. Physical and analytical properties of a stabilized electric field integral equation. *IEEE Transactions on Antennas and Propagation*, 52(2):362 – 372, Feb. 2004.

[42] W.C. Chew, J.-M. Jin, E. Michielssen, and J. Song. *Fast and efficient algorithms in computational electromagnetics*. Artech House, Boston, 2001.

[43] D. Schaubert, D. Wilton, and D. Glisson. A tetrahedral modeling method for electromagnetic scattering by arbitrarily inhomogeneous dielectric bodies. *IEEE Transactions on Antennas and Propagation*, 32(1):77–85, 1984.

[44] M.K. Li and W.C. Chew. Applying divergence-free condition in solving the volume integral equation. *Progress in Electromagnetics Research*, 57:311–333, 2006.

[45] L.E. Sun and W.C. Chew. A novel formulation of the volume integral equation for electromagnetic scattering. *Waves in Random and Complex Media*, 19(1):162–180, Feb. 2009.

[46] C-C. Lu, P. Ylä-Oijala, M. Taskinen, and J. Sarvas. Comparison of two volume integral equation formulations for solving electromagnetic scattering by inhomogeneous dielectric objects. *International IEEE AP-S Symposium, Charleston, USA*, 2009.

[47] M.C. van Beurden and S.J.L van Eijndhoven. Well-posedness of domain integral equations for a dielectric object in homogeneous background. *Journal of Engineering Mathematics*, 62:289–302, 2008.

[48] R. W. Ziolkowski. Propagation in and scattering from a matched metamaterial having a zero index of refraction. *Physical Review E*, 70:046608, Oct. 2004.

[49] M. Silveirinha and N. Engheta. Design of matched zero-index metamaterials using nonmagnetic inclusions in epsilon-near-zero media. *Physical Review B*, 75:075119, Feb. 2007.

[50] D. Zaluški, D. Muha, and S. Hrabar. Practical realization of DB unit cell. *Metamaterials 2012, The Sixth International Congress on Advanced Electromagnetic Materials in Microwaves and Optics*, pages 499–501, 2012.

[51] D. Zaluski, D. Muha, and S. Hrabar. Towards experimental investigation of metamaterial-based DB surface in waveguide environment. *2012 6th European Conference on Antennas and Propagation (EUCAP)*, pages 2861–2864, 2012.

[52] I.V. Lindell, L. Bergamin, and A. Favaro. The class of electromagnetic P-media and its generalization. *Progress in Electromagnetics Research B*, 28:143–162, 2011.

[53] K.L. Wong and H.T. Chen. Electromagnetic scattering by a uniaxially anisotropic sphere. *IEE Proceedings H, Microwaves, Antennas and Propagation*, 139(4):314–318, Aug. 1992.

[54] C.-W. Qiu, L. W. Li, T.S. Yeo, and S. Zouhdi. Scattering by rotationally symmetric anisotropic spheres: Potential formulation and parametric studies. *Physical Review E*, 75(2):026609, 2007.

[55] I.V. Lindell, A. Sihvola, L. Bergamin, and A. Favaro. Realization of the D′B′ boundary condition. *IEEE Antennas and wireless propagation lettters*, 10:643–646, 2011.

Aalto-DD 109/2013

ISBN 978-952-60-5242-7
ISBN 978-952-60-5243-4 (pdf)
ISSN-L 1799-4934
ISSN 1799-4934
ISSN 1799-4942 (pdf)

Aalto University
School of Electrical Engineering
Department of Radio Science and Engineering
www.aalto.fi

BUSINESS + ECONOMY

ART + DESIGN + ARCHITECTURE

SCIENCE + TECHNOLOGY

CROSSOVER

DOCTORAL DISSERTATIONS